Temperatures in Northern Greenland from 1952 to 2019 and Water Isotope Data from the Hans Tausen Ice Core

Ying Yu
Supervisor: Bo Møllesøe Vinther

2021/5

Abstract

The climate in the Arctic region is changing rapidly, but for northern Greenland climate records are sparse and discontinuous. To investigate climate evolution since the 1950s available temperature observations are compiled into two continuous series from northern Greenland. Interestingly, these new series show rapid warming in recent decades, with the temperature rise in the northernmost location being the largest in all of Greenland. The new temperature series are also compared to water isotope data from the ice core drilled through the Hans Tausen Ice Cap in 1995. These ice core data are influenced by both surface melt and firn diffusion, but after careful data treatment annual average accumulation and isotope data are recovered. Surprisingly, an inverse relationship between summer temperature and accumulation rate is found, suggesting higher temperatures are associated with reduced accumulation until 1995.

Keywords

Hans Tausen ice cap, temperature, isotope data, diffusion, accumulation rate

Contents

Introduction **8**

Temperature records **12**

2.1 The original data 12
2.2 Homogenizing the Alert and 4310 station data 15
2.2.1 A complete Alert records 15
2.2.2 A complete 4310 records 16
2.3 Regression work and results 19

Isotope Data **25**

3.1 Original isotope data. 25
3.2 Diffusion theory 28
3.3 Removing the noise from melt layers 32
3.3.1 Maximum entropy method 33
3.3.2 Result after infilling with MEM generated data 35
3.4 Deconvolution and result 35

The Relationship between Isotope Data, Temperature and Accumulation Rate **43**

4.1 Using the deconvoluted data to calculated annual average $\delta^{18}O$ values 43
4.2 Using the original data to calculate annual average $\delta^{18}O$ values 45
4.3 Including the 1983 and 1963 reference horizons in the dating . 46
4.4 Isotope data , temperature, and accumulation rate 48

Discussion **51**

5.1 Temperature 51
5.2 Isotope data 54

Conclusion **58**

Bibliography **61**

List of Tables

2.1 The general time periods recorded by the stations 13
2.2 The correlation coefficient between 4301 and other stations for different months 15
2.3 The correction calculation for Ua Alert 16
2.4 The relationship between Tm and T12 for 4310 17
2.5 The correlation coefficients for 4310 18
2.6 The parameters used in regression for 4310 and the correlation coefficients between original data and new data 18
2.7 The parameters used in regression for 4301 and the correlation coefficients between original data and new data 19
2.8 The parameters used in regression for 4301 and the correlation coefficients between original data and new data(only based on 4310) 20
2.9 The decadal mean annual temperature for the four stations . 23
2.10 The decadal mean seasonal temperature for station 4301 . . . 23
2.11 The decadal mean seasonal temperature for station 4310 . . . 24

3.1 The age-depth reference horizons for the Hans Tausen Ice Core[9] 26
3.2 The correlation coefficients between $\delta^{18}O$ and temperature record at station 4301. No values are with significance as the 10% significance level 27
3.3 The first assumption for three sections 38
3.4 The final parameters for three sections. 38
3.5 The 90% confidence interval for three parameters. 39

4.1 The correlation coefficients between deconvoluted $\delta^{18}O$ and temperature record at station 4301 and 4310, based on a time scale only taking into account the 1947 reference horizon. . . 44
4.2 The correlation coefficients between original $\delta^{18}O$ and temperature record at station 4301 and 4310. 45

4.3 The correlation coefficients between deconvoluted $\delta^{18}O$, original $\delta^{18}O$ and temperature record at station 4301 and 4310. 47
4.4 The correlation coefficients between deconvoluted $\delta^{18}O$, original $\delta^{18}O$ and accumulation rate. The coefficient with underline means 10% significant level, and coefficient in blackbody means 5% significant level. 50
4.5 The correlation coefficients between accumulation rate and temperature record at station 4301 and 4310. The coefficient in blackbody means 5% significant level. 50

5.1 The decadal temperature rise from 1979 to 2018 for stations from Greenland. 52

List of Figures

1.1 Trends in Arctic temperature and sea-ice cover. a, Near-surface air temperature (T2m) trend (°C per decade) over 1979–2018 from ERA-Interim[11][1]. b, Sea-ice concentration trend (percentage per decade) over 1979–2018 from ERA-Interim[11][1]. The trends are calculated for the entire 40-yr period and expressed as the change per decade. The red dots indicate the positions for Hans Tausen Ice Cap, and black dots indicate the position for danish meteorological stations. 8

1.2 The map of northern Greenland, including the position of the Hans Tausen Ice Cap. 9

2.1 The positions of temperature stations 13

2.2 The original annual averaged temperature for four stations(annual averages only calculated when all data for 12 months are available) 14

2.3 The annual averaged temperature for 4301 and 4310 21

2.4 The spring averaged temperature for 4301 and 4310 21

2.5 The summer averaged temperature for 4301 and 4310 22

2.6 The autumn averaged temperature for 4301 and 4310 22

2.7 The winter averaged temperature for 4301 and 4310 23

3.1 The original isotope data from Hans Tausen Ice Cap 25

3.2 The relationship between isotope value and time before and after calculating the annual averaged value 26

3.3 The comparison between isotope curve and temperature curve. The solid line is the annual averaged value, and the dashed line is the smoothed value after triangular filter. 27

3.4 Schematic description of the ice flow model used for flow calculation near the ice divide. 29

3.5 The result after infilling data with MEM. 35

3.6 The power spectrum comparison between before and after removing melting noise for the depth 0-2.79m. 36

3.7 The power spectrum comparison between before and after removing melting noise for the depth 2.79m-8.28m. 36
3.8 The power spectrum comparison between before and after removing melting noise for the depth 8.28m-11.76m. 37
3.9 The regression for the first section and the region for 90% confidence interval. 39
3.10 The regression for the second section and the region for 90% confidence interval. 40
3.11 The regression for the third section and the region for 90% confidence interval. 40
3.12 The re-corrected analytical diffusion length for the upper 11.76m ice core. 41
3.13 The final deconvolution result for isotope data for top 11.76m ice core 42

4.1 The annual layers based on the deconvolution and 1947 time point. 44
4.2 The annual layers in original data only based on 1947 time point. 45
4.3 The annual layers in the deconvoluted data based on 1983, 1963 and 1947 reference horizons. 46
4.4 The annual layers in original data based on 1983, 1963 and 1947 reference horizons. 47
4.5 The annual layers in deconvoluted data only based on 1947 time point in ice depth under the ice depth reference system. . 48
4.6 The annual layers in deconvoluted data based on 1983, 1963 and 1947 time points under the ice depth reference system. . . 49
4.7 The determined accumulation rate. 49

5.1 The locations for meteorological stations in south and north Greenland. Data from stations indicated with blue circles have been complied in this study. 52
5.2 The annual temperature averages at stations 4202, 4211, 4221, 4250, 4272 (mainly west coast), and the dashed lines are the corresponding linear regressions used to calculate the rate of temperature change in Tab. 5.1. 53
5.3 The annual temperature averages change at station 4320, 4339, 4360, 4301, 4310(mainly east coast), and the dashed lines are the corresponding linear regression used to calculate the rate of temperature change in Tab. 5.1. 53

5.4 Maps of annual and seasonal surface air temperature trends based on meteorological station data. Statistically significant (95% confidence level) trends are marked by larger circles. . . 55
5.5 Arctic sea ice extent anomalies compared to the average from 1979 to 2015 in August. 56
5.6 Arctic sea ice extent anomalies compared to the average from 1979 to 2015 in December. 56

1. Introduction

As extreme weather occurs worldwide, people pay more and more attention to climate change, especially around polar regions, where climatic conditions change rapidly. Hence, We focus on the Arctic in this thesis.

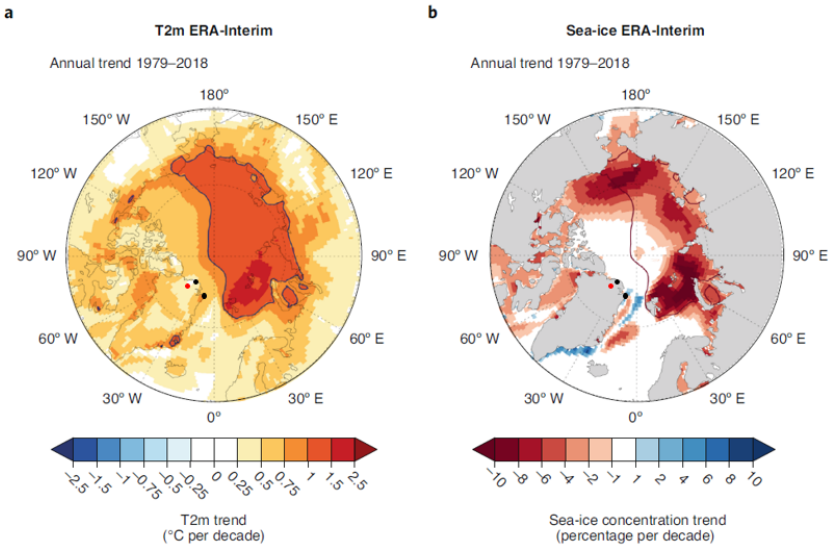

Figure 1.1: Trends in Arctic temperature and sea-ice cover. a, Near-surface air temperature (T2m) trend (°C per decade) over 1979–2018 from ERA-Interim[11][1]. b, Sea-ice concentration trend (percentage per decade) over 1979–2018 from ERA-Interim[11][1]. The trends are calculated for the entire 40-yr period and expressed as the change per decade. The red dots indicate the positions for Hans Tausen Ice Cap, and black dots indicate the position for danish meteorological stations.

(Figure adapted from[12])

In Fig. 1.1a, we can see that during 1979-2018, the surface temperatures experienced a considerable increase, especially the area contoured by blue and maroon lines, which shows an increasing trend greater than 1 °C per decade. This means during the past 40 years, there is a big area in the Arctic that has warmed up by more than 4 °C. From the isotope data from

Greenland ice cores, one remarkable thing that should be noticed is that only D-O events and the glacial termination equal the present-day warming in the Arctic[12]. From Fig. 1.1b, we can notice a massive amount of melting of sea ice associated with the increase in surface temperature. During summer, the melting of sea ice can cause more solar radiation to be absorbed by the sea and result in the Arctic warming up even further. While during winter, increased latent heat is released to the atmosphere from the open ocean. If we don't take any action to stop global warming, the ice sheet on Greenland will melt totally , which may cause about 7m global mean sea level rise[13].

The Antarctic is located on a continent, so we can drill ice cores to look into the climate change in the past hundreds of thousands of years. But for the Arctic, whose main part is made up of sea ice, this method is impossible. So we need to try some indirect way to get the information about Arctic climate change from areas around the Arctic Ocean.

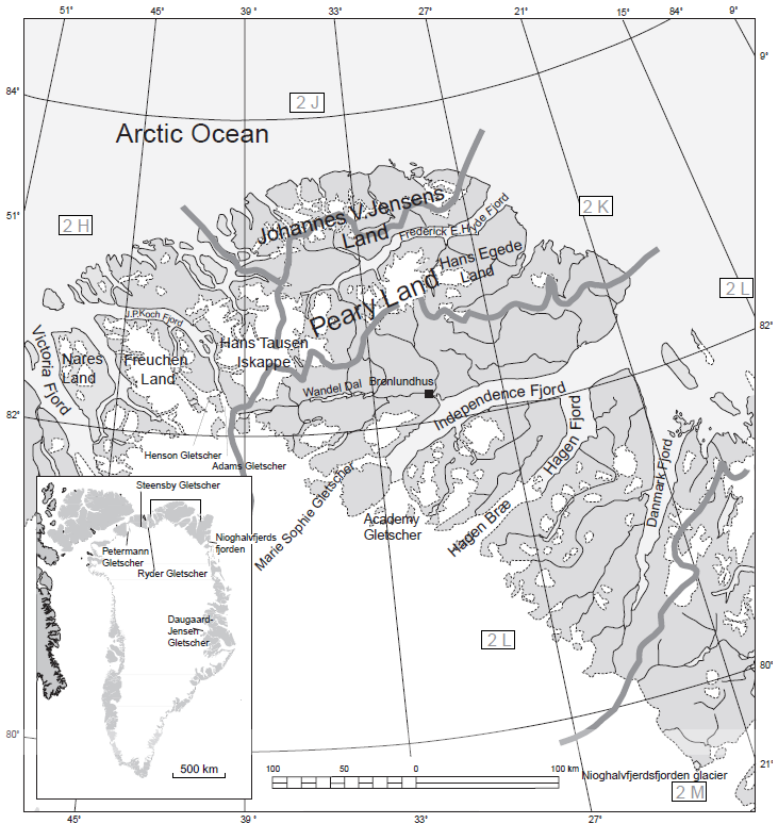

Figure 1.2: The map of northern Greenland, including the position of the Hans Tausen Ice Cap.

(Figure from[24])

When scientists analysed models used to simulate the future warming around the Arctic, they found that only the models with high climate sensitivity can reproduce the observed warming rate of over 1 degree per decade for the Arctic Ocean[12]. This phenomenon reflects the fact that the Arctic is more sensitive to climate change than other regions. So we can't research Arctic climate only based on model simulations. We still need some objective evidence to infer Arctic climate change.

Greenland is near the Arctic, but in the European Community Earth System Model under the extended representative concentration pathway (RCP) 8.5 scenario, the simulated future warming for the Greenland Ice Sheet is at a substantially slower rate that does not exceed the 1 degree per decade. This implies that an abrupt warming trend in the Arctic may not be reflected in the rate of warming in the Greenland Ice Sheet interior[12]. So we need some ice core from a place close to the Arctic Ocean to help us learn more about past Arctic climate change.

The Hans Tausen Ice Cap is an interesting candidate for obtaining information on past climatic conditions in the Arctic. It is the second largest ice cap in Northern Greenland, covering 4208 km^2. It is not only one of the northernmost ice caps in the world, but also one of the few which is close to the Arctic Ocean[22] [21].

Then, from Fig. 1.2, we can see that Hans Tausen Ice Cap is isolated from the Greenland Ice Sheet. Some evidence shows that the Hans Tausen Ice Cap was confluent with the Greenland Ice Sheet to the south during the last glaciation. However, this phenomenon ended during the last deglaciation, with the regression of ice cap, Hans Tausen Ice Cap separated from the Greenland Ice Sheet by 7200 BP[16]. This isolated position makes the ice core from Hans Tausen independent from the ones from Greenland Ice Sheet.

Moreover, in 1961, Langway pointed that the major source of moisture must be from the open water area among the pack ice and leads along the coastal regions from the northern direction[17].

All the three reasons: 1) Close location to the Arctic Ocean; 2) Separation from the Greenland Ice Sheet; 3) Water vapor sources from the north, make the Hans Tausen Ice Cap as an obvious location to study past climate change for the Arctic Ocean.

The ice core we use in this project was drilled in 1995, and its length is almost 350m, reaching bedrock under the Hans Tausen Ice Cap. But not all the ice core pieces are measured with high resolution. In this project, we only use the first 22m ice core pieces with isotope data for every 0.025m and covering the period from 1873 to 1995. However, due to a lack of continuous and homogenized temperature data from Northern Greenland, no one have made a detailed local analysis of the relationship between isotope data and

temperatures before. So we want to explore this relationship in detail.

In chapter 2, because the original temperature records have many gaps, I started working on compiling two continuous temperature records from northern Greenland. In chapter 3, the water isotope data from the Hans Tausen Ice Core are corrected for diffusion and melt effects to facilitate annual layer counting. Then chapter 4 is about the comparison between temperature observations, water isotope data, and accumulation rate data. The latter two being based on the new layer count. In chapter 5, the main results of the thesis are discussed and compared to climate change across the Arctic. Chapter 6 presents the main conclusions of the thesis.

2. Temperature records

There is no meteorological station on Hans Tausen Ice Cap, but there are some stations in Northern Greenland.

The Danish Meteorological Institute has maintained stations in northern Greenland to get the meteorological data from 1950s up to present. And there are some main stations that we will look into in this article, and their positions are shown in Fig.2.1. The numbers for the stations are 04301[8], 04310[7]. And stations 04320[7], Alert Ua and Alert Climate[18](because the two Alert station are in the same position, they will be called as Alert in the following article), even though they are not in the Northern Greenland, they can play an important role in filling out gaps in the Northern Greenland series, so the position of Alert is also indicated on the map. From the map we can see that station 4301 is in the closest position to the Hans Tausen Ice Cap, so our target in this chapter is to reconstruct a continuous temperature record for 4301.

2.1 The original data

I got the original data from the Danish Meteorological Institute[7][8]. Station 4301 recorded temperature 8 times a day before 2009.8, at 0am, 3am, 6am, 9am,12am, 3pm, 6pm, and 9pm. And after 2009.8, it began to record 24 times per day at every hour. Station 4310 recorded 8 times a day before 2008.8, and recorded every hour after 2008.8. Station 4320 recorded temperature 8 times before 1996.8, and recorded temperature at every hour after 1996.8. During some intervals , the stations may have only 2 temperature measurements a day, or gaps within a month. For a reliable monthly averaged temperature, I only calculated the mean temperature values for months with data for over 20 days and over 90 measurements. And as a result, different stations cover different time periods. The general time periods covered by the stations are listed in the table 2.1.

The annual mean temperature for 4301, 4310, 4320, and Alert are shown in Fig 2.2. I set 04301 as the target station, and calculated the correlation coefficient between 4301 and other stations for different months, which is shown

Figure 2.1: The positions of temperature stations (Figure adapted from [2])

Station name	Recording time period
04301 (Kap Morris Jesup)	1980.7-2005.11, 2009,8-2019.12
04310 (Station Nord)	1952.6-1972.6, 1975.9-2019.12
04320 (Danmarkshavn)	1949.1-2019.12
Alert Ua	1950.10-2006.12
Alert Climate	2004.7-2020.9

Table 2.1: The general time periods recorded by the stations

in table 2.2. And the station combined Alert is the Alert data calculated in section 3.1, a combination of Alert Ua and Alert Climate.

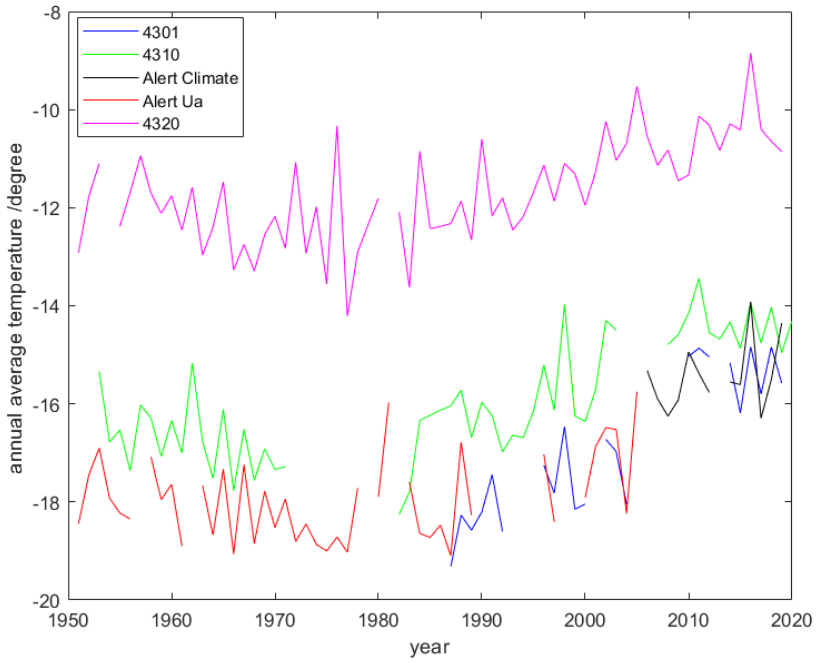

Figure 2.2: The original annual averaged temperature for four stations(annual averages only calculated when all data for 12 months are available)

From these figures and table we can see:

1) The averaged temperatures are influenced by the latitude. 4301, as the station with the highest latitude, has the lowest mean temperature. While the lower latitude station 4320 has a higher mean temperature.

2) Stations, 4310 and Alert, that are closer to 4301, generally have higher correlation coefficients, which means their temperatures are more closely related to each other . While station 4320, further from 4301, has lower correlation coefficients, which means their temperature are not strongly related to each other.

3) There are several big gaps in the 4301 temperature record. But the records for Alert, and 4310 are more complete, and the correlation coefficients with 4301 are relatively high. So we can use the data from the other two stations to get an approximate temperature record at 4301 by doing regression.

Correlation Coefficient with 4301 for different months	Station name		
	04310	04320	Combined Alert
JAN	0.852	0.484	0.782
FEB	0.870	0.619	0.875
MAR	0.828	0.396	0.854
APR	0.762	0.330	0.892
MAY	0.818	0.765	0.735
JUN	0.684	0.585	0.700
JUL	0.461	0.352	0.481
AUG	0.452	0.406	0.689
SEP	0.576	0.408	0.815
OCT	0.794	0.596	0.895
NOV	0.877	0.680	0.931
DEC	0.855	0.588	0.787

Table 2.2: The correlation coefficient between 4301 and other stations for different months

2.2 Homogenizing the Alert and 4310 station data

Because station 4310 and Alert have high correlation coefficient with 4301. The main idea to get a continuous temperature record at 4301 is doing the regression analysis with 4310 and Alert station, expressed as

$$T_{4301} = a \times T_{4310} + b \times T_{Alert} + c \tag{2.1}$$

But we need to make the temperature record for 4310 and Alert as complete and homogeneous as possible before proceeding with such a regression.

2.2.1 A complete Alert records

The temperature records at station Alert, station Alert Ua and Alert Climate are with the same latitude and longitude(82.5000N, 62.3333W), and there is a overlap period from 2004.7 to 2006.12, but their temperature records are not with the same value. Because station Alert Climate is a relatively new established station, we thought its record was more reliable, so Bo did the following correction to correct the data from Alert Ua .

$$\Delta T1 = T_{ClimateAlert} - T_{4301} \tag{2.2}$$

$$\Delta T2 = T_{UaAlert} - T_{4301} \tag{2.3}$$

$$Correction = \Delta T1 - \Delta T2 \tag{2.4}$$

$$T_{Alert} = T_{UaAlert} + Correction \tag{2.5}$$

And the results are shown in table 2.3. By doing the correction, and combining the two data versions together, we get a relatively complete temperature record for Alert from 1951 to 2019.

Month	$\Delta T1$	$\Delta T2$	Correction
JAN	-0.43	-0.41	-0.02
FEB	-1.85	-0.08	-1.77
MAR	-0.64	0.02	-0.66
APR	-0.96	-0.34	-0.62
MAY	-1.46	-0.71	-0.75
JUN	0.86	0.44	0.42
JUL	2.23	1.69	0.54
AUG	1.51	1.17	0.34
SEP	0.13	0.67	-0.55
OCT	0.22	0.81	-0.59
NOV	-0.02	0.67	-0.69
DEC	-0.66	-0.06	-0.602

Table 2.3: The correction calculation for Ua Alert

2.2.2 A complete 4310 records

It should be noted that while there is a gap for 4310 from 1975.9 to 1981.11, this is not because the station stopped working. Actually, the station still kept recording the temperature at 12am and 6pm but two daily data points are not enough to calculate daily mean temperature directly. So we still have some continuous temperature record for 4310, but need to take into account the diurnal cycle. The change of temperature over a day has an average a regular pattern. Around 6am, there is the lowest temperature for a day, but around 2pm, there is the highest temperature, and this is called the temperature diurnal cycle. So we can infer the mean temperature for a day from the temperature at a specific time, for example at 12am. For station 4310, I calculated the correlation coefficients between T_m (mean temperature for a day) and T_{12} (temperature at 12am), the difference between T_m and T_{12}, and the standard deviation for the difference for 37 years. The calculating results are listed in table 2.4. From the table we can see that

1) T_m and T_{12} are highly related to each other (high correlation coefficients).

2) The differences for T_m and T_{12} are different for different month, but they do not change so much along time. Then we can calculate T_m from T_{12} for the time period 1975.9-1981.11.

Month	Difference (Tm-T12)	Standard deviation	Correlation coefficient
JAN	0.093	0.346	0.994
FEB	-0.047	0.317	0.997
MAR	-0.408	0.400	0.988
APR	-0.517	0.351	0.992
MAY	-0.476	0.242	0.994
JUN	-0.419	0.286	0.981
JUL	-0.391	0.223	0.989
AUG	-0.420	0.246	0.977
SEP	-0.319	0.294	0.986
OCT	0.001	0.225	0.996
NOV	0.024	0.275	0.996
DEC	0.045	0.375	0.992

Table 2.4: The relationship between Tm and T12 for 4310

For the rest gaps in data from 4310, we did a regression analysis. Because station Alert and station 4320 have data back to 1950s, they can be considered to be as the bases to do regression. So I calculated the correlation coefficients to know whether 4310's temperature is influenced by Alert and 4320. From table 2.5, the correlation coefficients for both two stations are high enough to say that the temperature from the two places can influence the temperature in 4310.

Then I did the regression in MATLAB program, the regression formula for 4310 can be expressed as

$$T_{4310} = a \times T_{4320} + b \times T_{Alert} + c \tag{2.6}$$

After the regression, the values for parameters a, b, c and the correlation coefficients between original data and new data are shown in table2.6.

Up to now, we got the relatively complete data for both Alert station and 4310 station, but one thing should be noticed is that there are still some scattered months in the two stations that do not have data, and the influence from them will be mentioned in next chapter.

Month	Between 4310 and Alert	Between 4310 and 4320
JAN	0.724	0.782
FEB	0.701	0.788
MAR	0.736	0.783
APR	0.733	0.767
MAY	0.751	0.835
JUN	0.614	0.621
JUL	0.683	0.395
AUG	0.425	0.513
SEP	0.618	0.858
OCT	0.757	0.840
NOV	0.759	0.831
DEC	0.699	0.735

Table 2.5: The correlation coefficients for 4310

Month	a	b	c	Correlation Coefficients
JAN	0.579	0.523	0.159	0.882
FEB	0.618	0.399	-1.718	0.903
MAR	0.729	0.384	-0.626	0.902
APR	0.678	0.451	0.174	0.905
MAY	0.872	0.249	-1.106	0.858
JUN	0.441	0.353	-0.480	0.702
JUL	0.135	0.699	0.435	0.671
AUG	0.478	0.277	0.626	0.571
SEP	0.973	0.224	-2.271	0.897
OCT	0.608	0.374	-3.414	0.926
NOV	0.502	0.388	-3.074	0.916
DEC	0.607	0.523	1.101	0.866

Table 2.6: The parameters used in regression for 4310 and the correlation coefficients between original data and new data

2.3 Regression work and results

By doing the preparation work above, we now have enough data for 4310 and Alert to do regression for 4301.

The regression analysis for 4301 on the base of 4310 and Alert is expressed in equation 2.1, $T_{4301} = a \times T_{4310} + b \times T_{Alert} + c$, and the values for parameters a,b,c and the correlation coefficients between original data and new 4301 data is shown in table 2.7.

Month	a	b	c	Correlation Coefficients
JAN	0.664	0.416	1.302	0.891
FEB	0.646	0.530	4.895	0.943
MAR	0.558	0.631	5.056	0.894
APR	0.399	0.717	2.735	0.936
MAY	0.614	0.343	-0.508	0.884
JUN	0.429	0.365	-0.863	0.774
JUL	0.144	0.183	0.472	0.510
AUG	0.042	0.504	-0.824	0.690
SEP	0.229	0.761	-0.494	0.835
OCT	0.268	0.7439	-0.254	0.903
NOV	0.436	0.780	4.711	0.956
DEC	0.595	0.457	0.861	0.899

Table 2.7: The parameters used in regression for 4301 and the correlation coefficients between original data and new data

But as mentioned in section 2.2.2, there are still some scattered months missing data both for 4310 and Alert, so we can not get a really complete record for 4301 through this regression. Then we need to consider to only do regression based on one station. For the following months: 1957.2, 1962.9, 1979.10, 1979.11, 1982.1, 1995.1, 2013.2, they only have data from 4310 but not Alert, so I did regression only based on 4310.

$$T_{4301} = a \times T_{4310} + b \tag{2.7}$$

The parameters and the correlation coefficients between original and new data are listed in table 2.8

Then the resulted new temperature records for 4301, and 4310 are shown in Fig. 2.3, Fig. 2.4, Fig. 2.5, Fig.2.6 and Fig. 2.7. In Fig. 2.3, if there are more than six months' data are from the measurements, the year is labeled with blue, otherwise, it is labeled with yellow. In Fig. 2.4, Fig. 2.5, Fig.2.6 and Fig. 2.7, if there are 2 months' data are from the measurements,

Month	a	b	Correlation Coefficients
JAN	0.974	-2.832	0.845
FEB	1.094	0.309	0.884
SEP	0.579	-4.419	0.501
OCT	1.011	-0.774	0.811
NOV	1.131	1.211	0.877

Table 2.8: The parameters used in regression for 4301 and the correlation coefficients between original data and new data(only based on 4310)

then the year is labeled with blue, otherwise it is labeled with yellow. The smoothed curves for both 4310 and 4301 are from Triangular filter, which can be expressed as

$$T_{mean,i} = \frac{T_{i-2} + 2 \times T_{i-1} + 2 \times T_{i+1} + 3 \times T_i + T_{i+2}}{9} \tag{2.8}$$

And for first and last items it can be calculated as

$$T_{mean,1} = \frac{3 \times T_1 + 2 \times T_2 + T_3}{6} \tag{2.9}$$

$$T_{mean,n} = \frac{T_{n-2} + 2 \times T_{n-1} + 3 \times T_n}{6} \tag{2.10}$$

And for the second and the second to last items, it can be calculated as

$$T_{mean,2} = \frac{2 \times T_1 + 3 \times T_2 + 2 \times T_3 + T_4}{8} \tag{2.11}$$

$$T_{mean,n-1} = \frac{T_{n-3} + 2 \times T_{n-2} + 3 \times T_{n-1} + 2 \times T_n}{8} \tag{2.12}$$

Table 2.9 lists the decadal mean temperatures for four stations.

From Fig. 2.3, Fig. 2.4, Fig. 2.5, Fig.2.6 and Fig. 2.7, we can see that

1) For both two stations, the annual averaged temperature goes higher and higher from 1953 to 2019 by about 4 degree, especially after 2000, the rising speed was much faster.

2) When we look into the seasonal temperature change, one interesting phenomenon comes up: summer temperature also rose but not so much. But the temperature for winter experienced an apparent rise, and the rising trend is more significant than the growing annual temperature trend. For example, from Tab. 2.9 and Tab. 2.10, at station 4301, the 10-year mean summer temperature only rose less than 1 degree, while 10-year mean winter temperature increased by almost 5°C, as a comparison, the 10-year mean annual

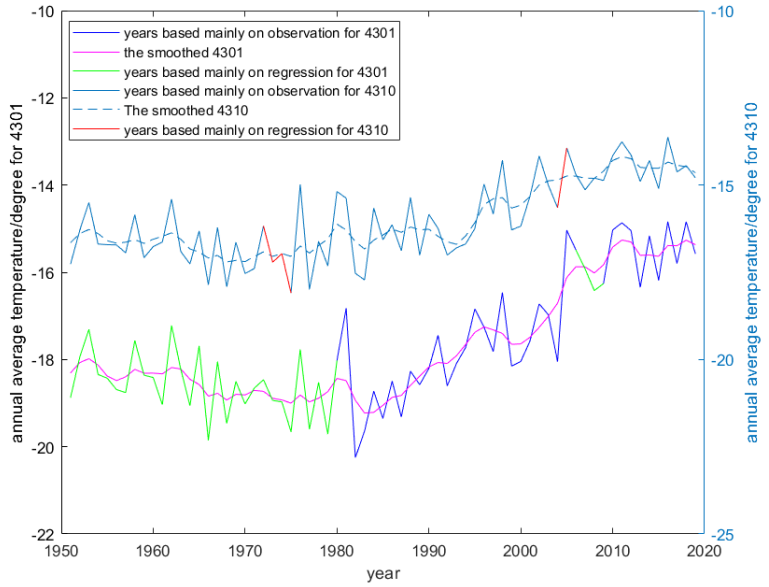

Figure 2.3: The annual averaged temperature for 4301 and 4310

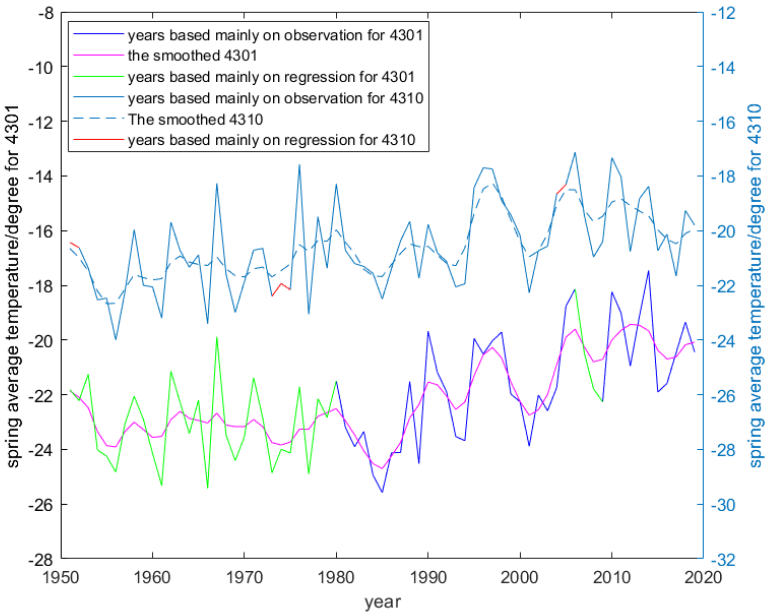

Figure 2.4: The spring averaged temperature for 4301 and 4310

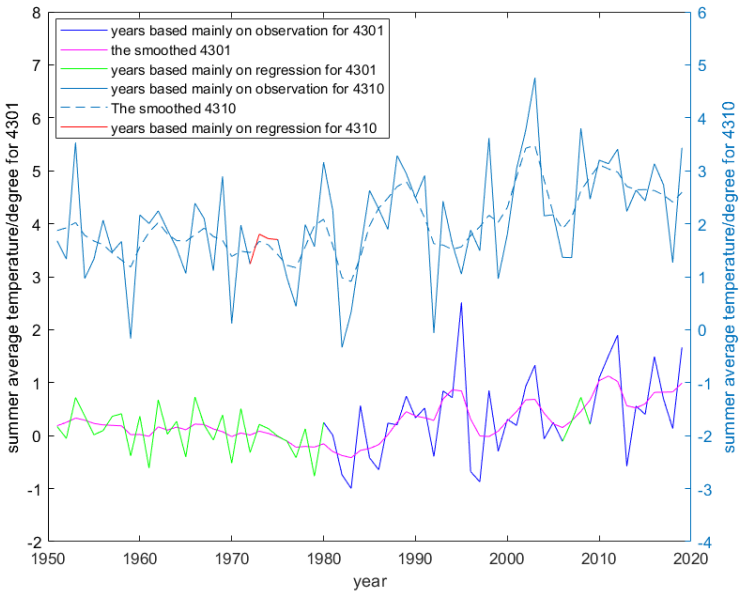

Figure 2.5: The summer averaged temperature for 4301 and 4310

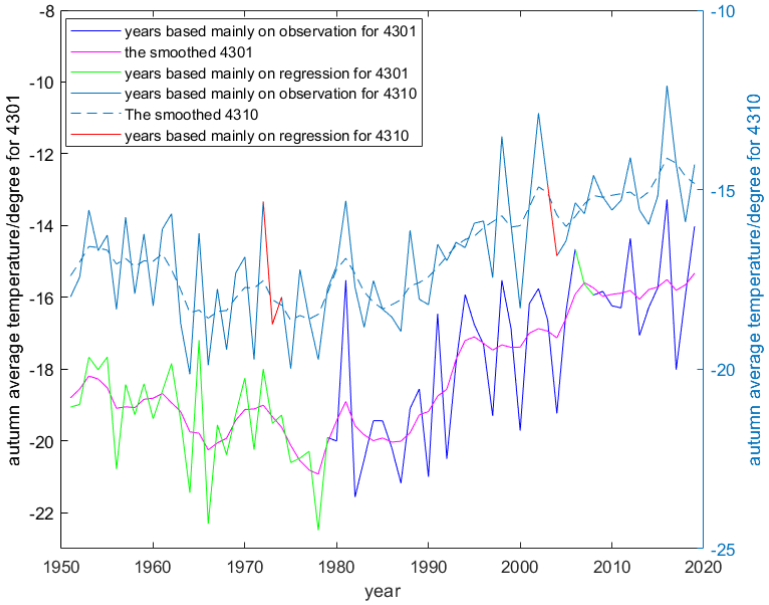

Figure 2.6: The autumn averaged temperature for 4301 and 4310

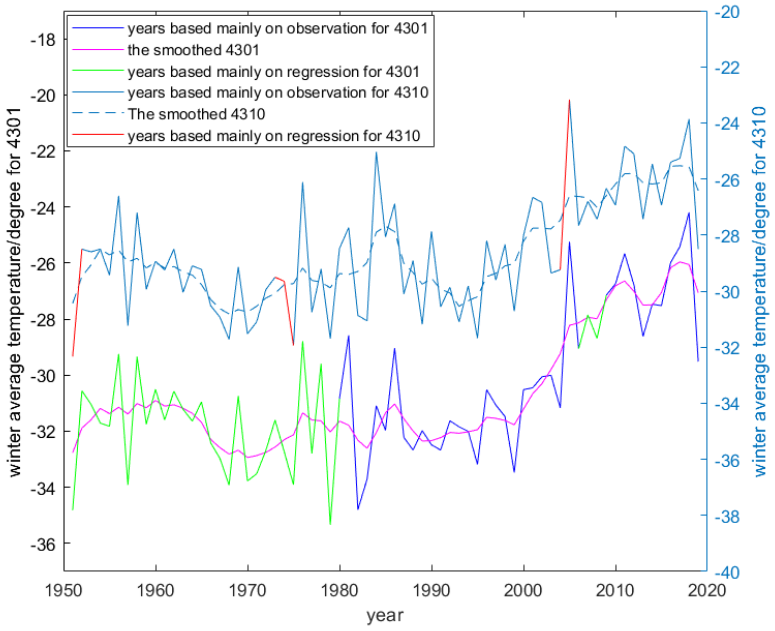

Figure 2.7: The winter averaged temperature for 4301 and 4310

Decade	4301	4310	4320	Alert
1951-1960	-18.3	-16.6	-11.8	-18.2
1961-1970	-18.6	-16.9	-12.5	-18.6
1971-1980	-18.8	-16.8	-12.4	-18.9
1981-1990	-18.8	-16.4	-12.1	-18.4
1991-2000	-17.6	-16.1	-11.8	-18.2
2001-2010	-16.3	-14.8	-10.8	-16.4
2011-2019	-15.4	-14.4	-10.3	-15.3

Table 2.9: The decadal mean annual temperature for the four stations

Decade	spring	summer	autumn	winter
1951-1960	-23.05	0.2	-18.8	-31.5
1961-1970	-23.1	0.1	-19.4	-32.0
1971-1980	-23.0	0.0	-20.1	-32.2
1981-1990	-23.5	-0.1	-19.6	-31.9
1991-2000	-21.5	0.4	-17.6	-31.8
2001-2010	-21.0	0.5	-16.2	-28.6
2011-2019	-20.0	0.9	-15.7	-26.8

Table 2.10: The decadal mean seasonal temperature for station 4301

Decade	spring	summer	autumn	winter
1951-1960	-21.8	1.6	-17.0	-29.1
1961-1970	-21.4	1.7	-17.8	-30.0
1971-1980	-20.8	1.7	18.2	-29.8
1981-1990	-21.0	1.9	-17.8	-28.8
1991-2000	-19.8	1.8	-16.4	-29.8
2001-2010	-19.6	2.8	-15.3	-27.0
2011-2019	-19.7	2.7	-14.7	-25.9

Table 2.11: The decadal mean seasonal temperature for station 4310

temperature increased for almost 3°C. So the global warm won't influence summer temperature so much, but winter will be warmed up significantly in Northern Greenland. The significant temperature rising in winter may come from the sea ice loss and needs to be discussed more in the later chapter. And the slower temperature rise in summer , and faster rise in winter at station 4310 are also reflected in Tab. 2.11.

Through all the above steps, one phenomenon that attracted my attention is that the correlation coefficients are much lower in summer (June, July, and August), no matter between which two stations. One possible reason for this is that because the temperature in summer did not change a lot through the 70 years for both four stations. As a result, it is not easy to say whether one station's temperature change can influence the other's temperature, then the correlation coefficients will be lower.

Because of the low correlation coefficients in summer, the regression results for summer may not be so accurate, which may affect the comparison we will proceed to make with the Hans Tausen Ice Core data.

3. Isotope Data

Our project's isotope data is from the ice core drilled in 1995 at the Hans Tausen Ice Cap. This ice core is as long as 350m, covering the history back to a few thousands years before present. But not all pieces of the ice core are of high resolution. Most of the ice core is with data for every 0.55m, while some parts are with data for every 0.025m, including the upper 22m.

In our project, we focus on these 22m, which covers the history from 1873 to 1995. This part is in high resolution yielding detailed information about the past climate change. But the original data is degraded by both melt layer and diffusion, so this chapter shows how we seek to restore the climate information despite these deficiencies.

3.1 Original isotope data.

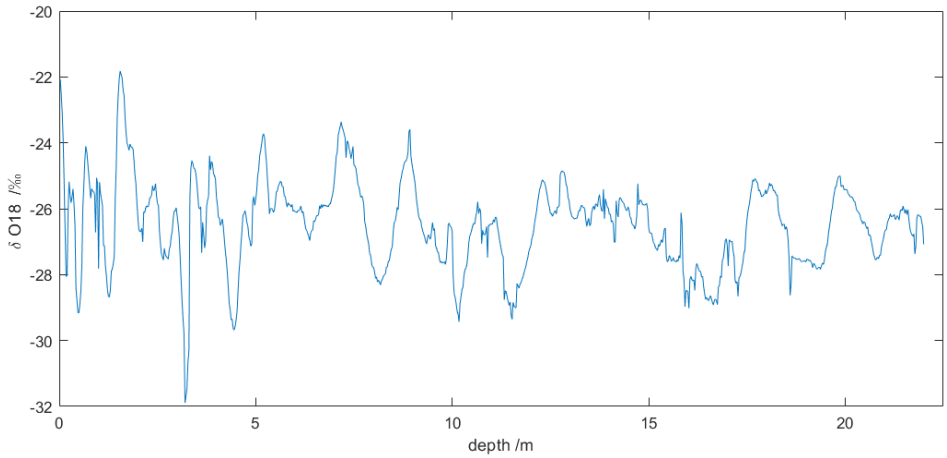

Figure 3.1: The original isotope data from Hans Tausen Ice Cap

Fig. 3.1 shows the original isotope data for the top 22m. But if we want to compare the isotope data with the temperature record, we need to change the x-axis to time. By the volcanic signal left in the ice core, we can decide

the age for some particular depth [9]. The depth-age relationship is shown in Tab. 3.1.

Age year	Depth (m)
1995	0
1983	2.79
1963	8.28
1947	11.76
1912	17.71
1873	23.15

Table 3.1: The age-depth reference horizons for the Hans Tausen Ice Core[9]

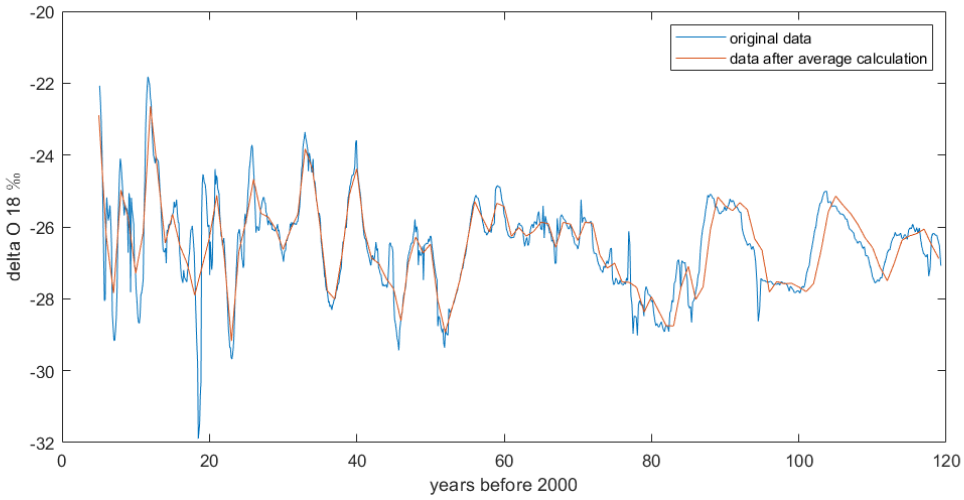

Figure 3.2: The relationship between isotope value and time before and after calculating the annual averaged value

By doing interpolation between these fixed points, we can get the approximate relationship between isotope value and time, which is shown in Fig. 3.2. Before comparing $\delta^{18}O$ with temperature, I calculated the annual average value for $\delta^{18}O$ firstly. The more recent the year is to 2000, the more isotope values were recorded in the ice core,

Then I use the annual average $\delta^{18}O$ curve to compare with the temperature at station 4301. And the result is shown in Fig. 3.3, and the correlation coefficients are shown in Tab. 3.2. But no matter the comparison is between annually averaged temperature, spring, summer, autumn, or winter mean

temperature, the result is hard to say that there is a relationship between $\delta^{18}O$ and temperature.

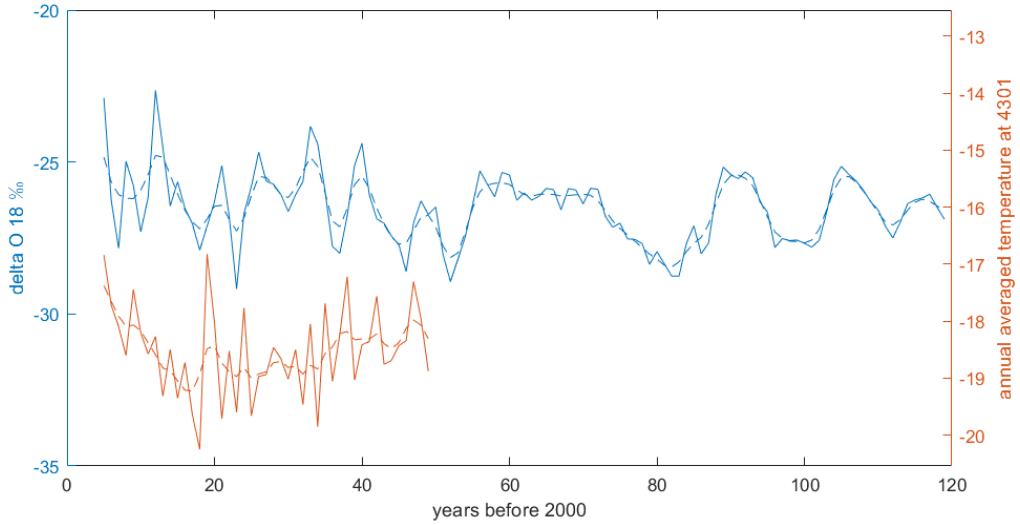

Figure 3.3: The comparison between isotope curve and temperature curve. The solid line is the annual averaged value, and the dashed line is the smoothed value after triangular filter.

	Spring	Summer	Autumn	Winter	Annual
Annual averaged $\delta^{18}O$	0.18346	0.2446	0.0250	-0.1766	0.0552
Smoothed $\delta^{18}O$	0.1067	0.2734	-0.0189	-0.3150	-0.0277

Table 3.2: The correlation coefficients between $\delta^{18}O$ and temperature record at station 4301. No values are with significance as the 10% significance level

We think this uncorrelated result maybe because of the low quality of isotope data, which means this data has been distorted by the natural process, like diffusion.

When we look into Fig. 3.1, firstly, we can notice that the deeper the data is, the smaller the amplitude is. This phenomenon comes from diffusion. Actually, for the ice core in the top 22m, most of it is made up of firn which is porous. And these air passages become the channel for isotope stored in the ice core to make thermodynamic diffusion motion. And this motion will smooth the curve. This diffusion process will be discussed more in the next section.

Secondly, when we look at details, we can find some huge leaps in this curve. For example, during the depth from 3.5m to 3.75m, from 8.85m to

8.95m, from 10.88m to 10.95m, and from 18.52m to 18.68m, we can see the isotope value changes a lot in a short interval. Usually, before or after diffusion, the isotope value should change gradually instead of being with a big jump. And this abnormal jump is from the melting phenomenon. The melting water will block the bubble channel for diffusion, so the diffusion process is stopped at the melting part, and the isotope stored in this melting part is isolated from other parts. So this isotope curve is distorted by the melting phenomenon. If we want to get the curve showing isotope data after normal diffusion motion, we need to delete the distorted parts firstly. And this process is shown in the later section.

Thirdly, because of the extremely low temperature in Northern Greenland, the air there is very dry, and the precipitation is also low at Hans Tausen Ice Cap. This means that not so much isotope information can be stored in the ice core and easily distorted by the past deposition processes, such as sastrugi. The relatively high correlation coefficient in summer between $\delta^{18}O$ and temperature may mean that the low precipitation concentrate in the summer.

At last, it is not accurate to decide the time of isotope data only from interpolation. If we want to know the exact age year for isotope data, it is better to count the annual layer firstly.

So for a better comparison work, it is needed to restore the distorted data firstly. Then try to count the annual layer. Lastly, compare the isotope data to temperature.

3.2 Diffusion theory

When snow falls on the ground, its density is lower than $300kg/m^3$ which means that it has much air inside. This air make channels for the molecules to do thermodynamic diffusion motion. As more snow falls, and under its gravity, the snow begins to be more compact, more air is expelled from the snow, and snow's density begins to rise to $550kg/m^3$, and the snow is transformed to firn. As the densification goes on, the air passages are closed off slowly to become air bubbles, which can still allow the diffusion process but much much slower. When firn's density reaches $917kg/m^3$, then firn is transformed to ice finally. During ice stage, there is almost no diffusion happens[6].

Because the isotope data we used is from the top 22m, which is made of snow, firn mostly and the density is lower than $800kg/m^3$[9], we only consider the diffusion that happens in snow and firn stages.

Before deriving the diffusion length, we should know the ice cap's flow

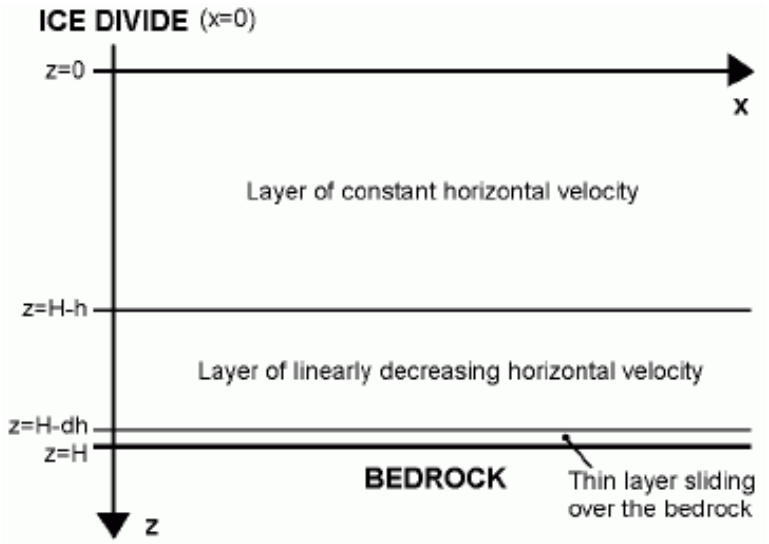

Figure 3.4: Schematic description of the ice flow model used for flow calculation near the ice divide.
(Figure from [19])

model and its assumptions. Fig. 3.4 shows the flow models introduced by Johnsen and Dansgaard[15]. In this model, z means the depth from the surface of the ice cap, H means the thickness of ice cap, h and dh are constants that can be determined from analysing the ice cap, and x means the distance from the ice divide. The depth is divided into three layers: 1) From 0 to H-h, the layer of constant horizontal velocity. 2) From H-h to H-dh, the layer of linearly decreasing horizontal velocity. 3) From H-dh to the bottom, a thin layer sliding over the bedrock. In the Hans Tausen Ice Cap, from the cap's thickness and movement profile, the depth of z=H-h is more than 50m. For our isotope data is from the top 22m, we only care the movement happening in the first layer.

The flow model is based on these assumptions:

1)The flow is two dimensional, both in the x-direction and in the z-direction.

2)The thickness of the ice sheet and the accumulation rate are constant both in time and along the flow direction.

3) The ice sheet is in a steady state.

4) There is no melting at the bottom of the ice sheet.

5) The horizontal velocity in the ice sheet can be expressed as :

$$u = \ U \cdot x, \quad 0 \leq z \leq H - h \tag{3.1}$$

In this equation, u means horizontal velocity. U can be expressed as

$$U = \frac{c}{H_{eff}}, \quad H_{eff} = H^* - \frac{1}{2}(h + dh)(1 - f_b) \tag{3.2}$$

c is the accumulation rate in meters of ice equivalent. f_b is the ratio between the bottom sliding velocity and the surface velocity.H^* is the ice sheet thickness in meters of ice equivalent.

And Bo M. Vinther, in his thesis[19], introduced the densification process in the Dansgaard-Johnsen flow model.

6) The density varies only with depth and is expressed as($z < H - h$):

$$\rho = \begin{cases} \rho_i \frac{R_0 e^{\rho_i k_0 z}}{1 + R_0 e^{\rho_i k_0 z}}, & R_0 = \frac{\rho_0}{\rho_i - \rho_0}, \quad \rho \leq \rho_c \\ \rho_i \frac{R_c e^{\rho_i k_1 (z - z_c) c_w^{-0.5}}}{1 + R_c e^{\rho_i k_1 (z - z_c) c_w^{-0.5}}}, & R_c = \frac{\rho_c}{\rho_i - \rho_c}, \quad \rho > \rho_c \end{cases} \tag{3.3}$$

ρ_0 means the density at the surface of ice sheet, ρ_i is the density for ice $917kg/m^3$, and ρ_c is $550kg/m^3$. c_w denotes the snow accumulation rate in meters of water equivalent. z_c is the depth at which $\rho = \rho_c$ and can be calculated by

$$z_c = \frac{\ln(\rho_c/\rho_0)}{\rho_i k_0} \tag{3.4}$$

k_0 and k_1 are two parameters, can be calculated by[6]

$$k_0 = f_0 \cdot 0.011 \cdot e^{\frac{-0.106}{k_B T}} \tag{3.5}$$

$$k_1 = f_1 \cdot 0.575 \cdot e^{\frac{-0.223}{k_B T}} \tag{3.6}$$

Where $k_B = 8.6167 \cdot 1 - ^{-5} ev/K$ is the Boltzmann constant, and the two factors $f_0 = 0.85, f_1 = 1.15$ are scaling constants introduced by Johnsen et al[10]. T is the local temperature in kelvin.

Based on these six assumptions, and considering the continuity equation for $z \leq H - h$, the vertical velocity w can be evaluated as

$$\begin{aligned} w(\rho) &= \frac{\rho_i c}{\rho} + \frac{U}{k_0 \rho} \ln(\frac{\rho_i - \rho}{\rho_i - \rho_0}) && \rho \leq \rho_c \\ w(\rho) &= \frac{\rho_i c}{\rho} + \frac{U}{k_0 \rho} \ln(\frac{\rho_i - \rho_c}{\rho_i - \rho_0}) + \frac{U c_w^{0.5}}{k_1 \rho} \ln(\frac{\rho_i - \rho}{\rho_i - \rho_c}) && \rho > \rho_c \end{aligned} \tag{3.7}$$

After calculating both horizontal and vertical velocity, we are approaching the diffusion length for one more step. The diffusion length can be gotten from Eq. 3.8[14], in which σ means the diffusion length, $\dot{\varepsilon_z}$ means the vertical strain rate in the ice, and Ω means diffusivity.

$$\frac{d\sigma^2}{dt} = 2\dot{\varepsilon_z}\sigma^2 + 2\Omega \tag{3.8}$$

The vertical strain rate can be determined from horizontal velocity and vertical velocity.

$$\dot{\varepsilon_z} = -\frac{du}{dx} - w\frac{d\rho}{\rho dz} \tag{3.9}$$

And the diffusivity can be calculated from[10]

$$\Omega = \gamma(1 - b\frac{\rho^2}{\rho_i^2})(\frac{1}{\rho} - \frac{1}{\rho_i}) \tag{3.10}$$

While b=1.3 and

$$\gamma = \frac{mp\Omega_a}{RT\alpha} \tag{3.11}$$

In Eq. 3.11, m is the molar weight for water, R is the gas constant, T is the temperature in kelvin, $\alpha = 0.9722 \cdot e^{\frac{11839}{T}}$[20] and p is the saturation vapor pressure in ice[10].

$$p = 3.454 \cdot 10^{12} \cdot e^{\frac{-6133}{T}} \tag{3.12}$$

Ω_a is the diffusivity of water vapor in air

$$\Omega_a = \frac{2110}{q}(\frac{T}{T_0})^{1.94}\frac{P_0}{P} \tag{3.13}$$

Here P is the pressure in atm, $T_0 = 273.15k$, and $P_0 = 1atm$, and q=1.0285[20]. Then the diffusion length in snow and firn can be calculated as

$$\sigma^2 = (\frac{\rho_n}{\rho})^2(\frac{\rho_i - \rho}{\rho_i - \rho_n})^\kappa \left[\frac{2\gamma}{Kc\rho_n^2\rho_i^2}(I - \frac{b}{\rho_i^2}II) + \sigma_n^2\right] \tag{3.14}$$

$$\rho_n = \begin{cases} \rho_0 & \rho_0 \leq \rho \leq \rho_c \\ \rho_c & \rho_c < \rho \leq 804.3kg/m^3 \end{cases} \tag{3.15}$$

$$\sigma_n = \begin{cases} 0 & \rho_0 \leq \rho \leq \rho_c \\ \sigma(\rho_c) & \rho_c < \rho \leq 804.3kg/m^3 \end{cases} \tag{3.16}$$

$$K = \begin{cases} k_0 & \rho_0 \leq \rho \leq \rho_c \\ k_1 c_w^{-0.5} & \rho_c < \rho \leq 804.3kg/m^3 \end{cases} \tag{3.17}$$

$$\kappa = \frac{2}{\rho_i H_{eff} K} \tag{3.18}$$

And I and II are

$$I = (\frac{\rho_i - \rho_n}{\kappa - 1})\left[\rho(\frac{\rho_i - \rho_n}{\rho_i - \rho})^{\kappa-1} - \rho_n - (\frac{\rho_i - \rho_n}{\kappa - 2})\left((\frac{\rho_i - \rho_n}{\rho_i - \rho})^{\kappa-2} - 1\right)\right] \tag{3.19}$$

$$II = (\frac{\rho_i - \rho_n}{\kappa - 1}) \left\{ \rho^3 (\frac{\rho_i - \rho_n}{\rho_i - \rho})^{\kappa-1} - \rho_n^3 - 3(\frac{\rho_i - \rho_n}{\kappa - 2}) \left[\rho^2 (\frac{\rho_i - \rho_n}{\rho_i - \rho})^{\kappa-2} - \rho_n^2 \right.\right.$$
$$\left.\left. -2(\frac{\rho_i - \rho_n}{\kappa - 3}) \left\{ \rho (\frac{\rho_i - \rho_n}{\rho_i - \rho})^{\kappa-3} - \rho_n - \frac{\rho_i - \rho_n}{\kappa - 4} \left[(\frac{\rho_i - \rho_n}{\rho_i - \rho})^{\kappa-4} - 1 \right] \right\} \right] \right\} \tag{3.20}$$

From all the above equations, we need the parameters for the density in ice(firn), which cen be gotten from [9], the local accumulation rate (c=0.11m/year[24]), the local temperature(T=-21°C[22]), local pressure (p=900 hPa, which is calculated from the Hans Tausen's elevation), and $H_{eff} = 300m$ (implied from this ica cap's altitude and movement profile) to calculate the diffusion length in this ice core, and the analytical diffusion length is shown in Fig. 3.12.

3.3 Removing the noise from melt layers

When we have the data only distorted by the diffusion process, and calculate the diffusion length, we can get the data before diffusion by deconvolution. But the isotope data from the Hans Tausen Ice Cap is also affected by melt layers, which will obstruct the diffusion process and result in the real diffusion length shorter than the theoretical one. So we can not calculate the diffusion length being shorter based on the theory in section 3.2 entirely. Therefore, we need another method to calculate the diffusion length.

Based on the power spectral density, we can imply the averaged diffusion length for a section of the isotope data. From the Eq.3.21 [10]

$$P(k) = P_0(k) exp(-k^2\sigma^2) \tag{3.21}$$

k is the wave number ($2\pi/\lambda$,λ is the wavelength), $P_0(k)$ is the spectral density of the profile without diffusion, $P(k)$ is the spectral density after diffusion, and σ is the diffusion length. But because there is some noise coming from measurement and melting phenomenon, in reality the equation should be rewritten as

$$P(k) = P_0(k) exp(-k^2\sigma^2) + n \tag{3.22}$$

Here n is the noise part.

So we can get the diffusion length by the following steps

1) Get the power spectral density for a section of data.

2) Calculate the averaged diffusion length for this section.

3) Calculate the theoretical diffusion length for this section.

4) Correct the theoretical diffusion length based on the averaged one to get the continuously changing diffusion length for the isotope data.

After we know the diffusion length, we can determine the original power spectral density at k wave number by

$$P_0(k) = P(k)exp(k^2\sigma^2) \tag{3.23}$$

From Eq. 3.3, we can see that the higher wave number is, the more its spectral density will be amplified. And the noise is with higher wave number than the isotope signal, so after deconvolution, noise's amplitude will be amplified so much that may overlay the isotope signal. So we need to weaken the noise signal as much as possible at first. We can not weaken the noise from measurement, but we can remove the noise from melting process.

By observing Fig. 3.1, we can find some pieces' isotope data changing dramatically, and these are from the melting distortion. So by deleting the distorted data and filling the data based on maximum entropy method, we can get the data almost without melting noise.

This section focus on how we remove the melting noise from the isotope data mainly.

3.3.1 Maximum entropy method

Besides Fourier transform, maximum entropy method(MEM) is another way to get the power spectral density for a profile, and much easier for people to use when there was a shortage of computer.

By using MEM, a set of data $x_1, x_2, ..., x_N$ with equal spacing Δt , then the power spectral density at frequency (f) can be calculated as[4]

$$P(f) = \frac{P_m \Delta t}{|1 - \Sigma_{n=1}^{m} a_{m,n} e^{-2\pi i f n \Delta t}|^2} \tag{3.24}$$

Parameters P_m and a_{mn} can be determined by the following steps.

Begin with m=0, then

$$P_0 = \frac{1}{N}\Sigma_{i=1}^{N} x_i^2 \tag{3.25}$$

When m=1

$$\begin{gathered} b_{1,1} = x_1 \\ b'_{1,N-1} = x_N \end{gathered} \tag{3.26}$$

$$b_{1,i} = b'_{1,i-1} = x_i \quad 2 \le i \le N-1 \tag{3.27}$$

$$a_{1,1} = 2\frac{\Sigma_{i=1}^{N-m} b_{1,i} b'_{1,i}}{\Sigma_{i=1}^{N-m}(b_{1,i}^2 + b'^2_{1,i})} \tag{3.28}$$

$$P_1 = P_0(1 - a_{1,1}^2) \tag{3.29}$$

When $m \geq 2$

$$\begin{aligned} b_{m,i} &= b_{m-1,i} - a_{m-1,m-1} \cdot b'_{m-1,i} \\ b'_{m.i} &= b'_{m-1,i+1} - a_{m-1,m-1} \cdot b_{m-1,i+1} \end{aligned} \tag{3.30}$$

$$a_{m,m} = 2\frac{\Sigma_{i=1}^{N-m} b_{m,i} b'_{m,i}}{\Sigma_{i=1}^{N-m}(b_{m,i}^2 + b_{m,i}'^2)} \tag{3.31}$$

$$P_m = P_{m-1}(1 - a_{m,m}^2) \tag{3.32}$$

$$a_{m,k} = a_{m-1,k} - a_{m.m} \cdot a_{m-1,m-k}, \quad 1 \leq k < m \tag{3.33}$$

The larger the parameter m is, the more accurate the power spectrum will be. With a small m, the curve of power spectrum is smooth.

Because in our project, the isotope data are equally distributed in space domain, Δt is the space interval, and f here is the wave number.

When we want to predict a given value s_i in a series $(s_1, s_2, ...s_M)$ with m parameters, then the forward prediction should be

$$s_i(pred) = \Sigma_{k=1}^{m} a_k s_{i-k} \tag{3.34}$$

The backward prediction should be

$$s_i(back - pred) = \Sigma_{k=1}^{m} a_k s_{i+k} \tag{3.35}$$

Then the forward prediction error is

$$f_i = s_i - s_i(pred) = s_i - \Sigma_{k=1}^{m} a_k s_{i-k} \tag{3.36}$$

The backward prediction error is

$$b_i = s_i - s_i(back - pred) = s_i - \Sigma_{k=1}^{m} a_k s_{i+k} \tag{3.37}$$

Then the mean error of the prediction model can be defined as

$$E = \frac{1}{2(M-m)}(\Sigma_{k=m+1}^{M} f_i + \Sigma_{i=1}^{M-m} b_i) \tag{3.38}$$

The MEM seeks to determine the m parameters in the model that cam make E minimized.

Actually, Andersen has proved that the parameters in Eq. 3.24 are the parameters that can minimize E, let $P_m = E, a_{m,n} = a_k$[4]. But in the Matlab script used in this project, a small modification is applied: The MEM parameters are based on two separate data sections instead of one [23], then the parameters are decided based on weighted average, by putting more weight on longer section.

3.3.2 Result after infilling with MEM generated data

I deleted 21 pieces of data. When using MEM, we need to decide the filter length, which describe the length of the data that we use to determine the prediction parameters. And in this project, I use 20 as the filter length.

The result and the comparison to the old data are shown in Fig. 3.5.

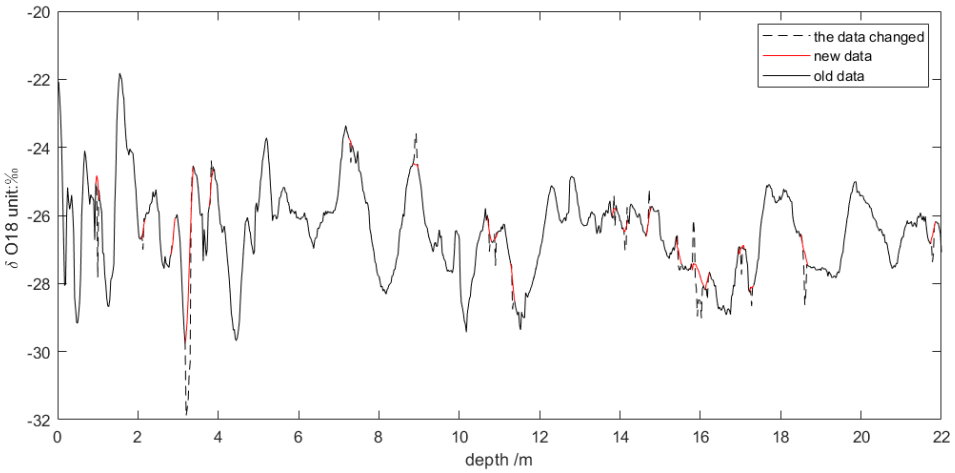

Figure 3.5: The result after infilling data with MEM.

Given that the temperature observations begin in the 1950s, I focused on the corresponding sections of the ice core. Hence, I divided the upper part of the isotope data into three sections according to Tab. 3.1. The first section covers the data from 1983 to 1995, the second covers the data from 1963 to 1983, the third covers the data from 1947 to 1963. Then I compared their power spectrum between before and after removing melting noise separately. The results are shown in Fig. 3.6, 3.7, 3.8. The unit for power spectrum is $(ppbw)^2$.

From these figures, we can see that the power spectrum at high wave number parts are weakened slightly, but low wave number part are not changed apparently.

3.4 Deconvolution and result

After getting the power spectral density for the three sections, we can make a regression to the power spectrum based on the Eq. 3.22.

In Eq. 3.22, $k = 2\pi/\lambda$, but when we calculate the power spectral density,

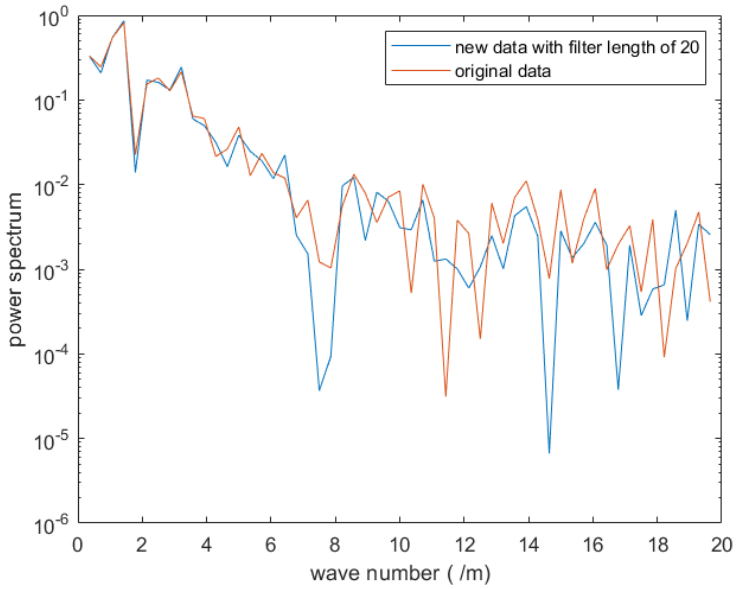

Figure 3.6: The power spectrum comparison between before and after removing melting noise for the depth 0-2.79m.

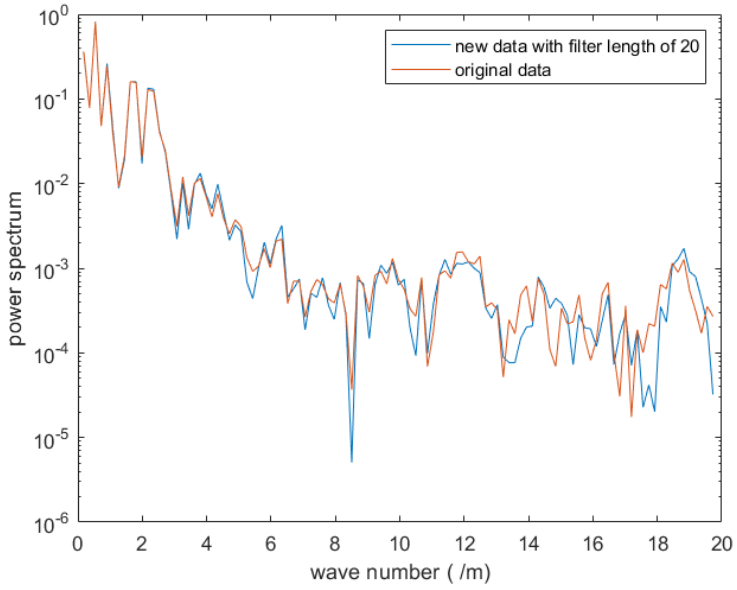

Figure 3.7: The power spectrum comparison between before and after removing melting noise for the depth 2.79m-8.28m.

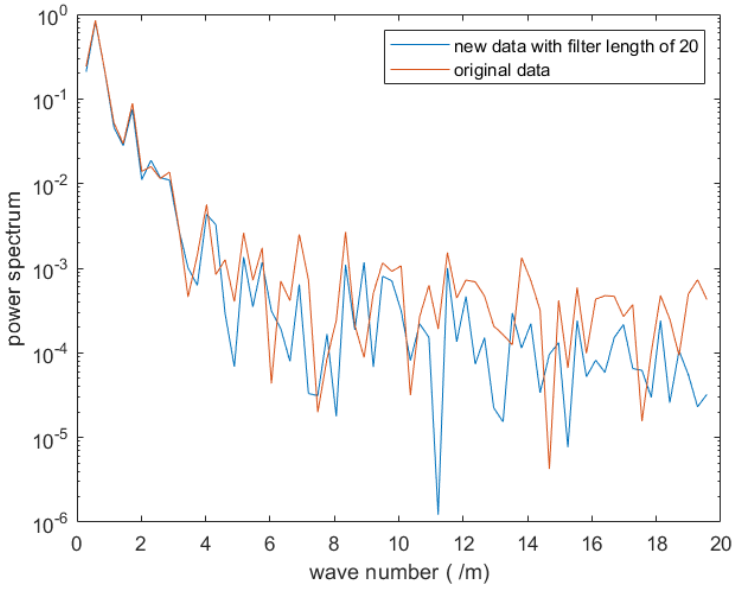

Figure 3.8: The power spectrum comparison between before and after removing melting noise for the depth 8.28m-11.76m.

we define $k = 1/\lambda$. Then the equation should be rewritten as

$$P = P_0 e^{-4\pi^2 k^2 \sigma^2} + n \tag{3.39}$$

Besides, for a better regression result, we put log to both sides in Eq. 3.39, then the equation is changed to

$$LP = \log_{10} P = \log_{10}(P_0 e^{-4\pi^2 k^2 \sigma^2} + n) \tag{3.40}$$

Among the three parameters,P_0, σ, n, it is important to get the values for σ and n. σ is the diffusion length we want to get, and n decides to which wave number the deconvolution should stop. To determine the parameters, I used Newton's Method.

$$\mathrm{G}\Delta\mathrm{m} = \mathrm{d} - g(\mathrm{m}^{(p)}) \tag{3.41}$$

$$\mathrm{m}^{(p+1)} = \mathrm{m}^{(p)} + \alpha\Delta\mathrm{m} \tag{3.42}$$

In which, m is the column for the parameters used in Eq. 3.40,

$$\mathrm{m} = \begin{bmatrix} P_0 & \sigma & n \end{bmatrix}^T \tag{3.43}$$

$\mathrm{m}^{(p)}$ is the pth guess for the parameters. d is the data, and $g(\mathrm{m}^{(\mathrm{p})})$ is the values gotten based on the pth guess for the parameters. α is a value between

1 and 0. The expression of matrix G is written as

$$G = \begin{bmatrix} \frac{\partial LP_1}{\partial P_0} & \frac{\partial LP_1}{\partial \sigma} & \frac{\partial LP_1}{\partial n} \\ \frac{\partial LP_2}{\partial P_0} & \frac{\partial LP_2}{\partial \sigma} & \frac{\partial LP_2}{\partial n} \\ \cdots & \cdots & \cdots \\ \frac{\partial LP_i}{\partial P_0} & \frac{\partial LP_i}{\partial \sigma} & \frac{\partial LP_i}{\partial n} \\ \cdots & \cdots & \cdots \\ \frac{\partial LP_n}{\partial P_0} & \frac{\partial LP_n}{\partial \sigma} & \frac{\partial LP_n}{\partial n} \end{bmatrix} = \begin{bmatrix} \frac{e^{-4\pi^2 k_1^2 \sigma^2}}{(P_0 e^{-4\pi^2 k_1^2 \sigma^2}+n)\cdot \ln 10} & \frac{P_0 e^{-4\pi^2 k_1^2 \sigma^2}\cdot(-8\pi^2 k_1^2 \sigma)}{(P_0 e^{-4\pi^2 k_1^2 \sigma^2}+n)\cdot \ln 10} & \frac{1}{(P_0 e^{-4\pi^2 k_1^2 \sigma^2}+n)\cdot \ln 10} \\ \frac{e^{-4\pi^2 k_2^2 \sigma^2}}{(P_0 e^{-4\pi^2 k_2^2 \sigma^2}+n)\cdot \ln 10} & \frac{P_0 e^{-4\pi^2 k_2^2 \sigma^2}\cdot(-8\pi^2 k_2^2 \sigma)}{(P_0 e^{-4\pi^2 k_2^2 \sigma^2}+n)\cdot \ln 10} & \frac{1}{(P_0 e^{-4\pi^2 k_2^2 \sigma^2}+n)\cdot \ln 10} \\ \cdots & \cdots & \cdots \\ \frac{e^{-4\pi^2 k_i^2 \sigma^2}}{(P_0 e^{-4\pi^2 k_i^2 \sigma^2}+n)\cdot \ln 10} & \frac{P_0 e^{-4\pi^2 k_i^2 \sigma^2}\cdot(-8\pi^2 k_i^2 \sigma)}{(P_0 e^{-4\pi^2 k_i^2 \sigma^2}+n)\cdot \ln 10} & \frac{1}{(P_0 e^{-4\pi^2 k_i^2 \sigma^2}+n)\cdot \ln 10} \\ \cdots & \cdots & \cdots \\ \frac{e^{-4\pi^2 k_n^2 \sigma^2}}{(P_0 e^{-4\pi^2 k_n^2 \sigma^2}+n)\cdot \ln 10} & \frac{P_0 e^{-4\pi^2 k_n^2 \sigma^2}\cdot(-8\pi^2 k_n^2 \sigma)}{(P_0 e^{-4\pi^2 k_n^2 \sigma^2}+n)\cdot \ln 10} & \frac{1}{(P_0 e^{-4\pi^2 k_n^2 \sigma^2}+n)\cdot \ln 10} \end{bmatrix} \tag{3.44}$$

According to Tikhonov Method, because this is an overdetermined problem, Δm should be determined by

$$\Delta \mathrm{m} = (\mathrm{G}^T \cdot \mathrm{G} + \mathrm{I})^{-1} \cdot \mathrm{G}^T \cdot (\mathrm{d} - g(\mathrm{m}^{(p)})) \tag{3.45}$$

So the steps to get the approximations for the parameters should be:
1) Make the first assumption for P_0, σ, n.
2) Calculate the matrix G and $g(m^{(1)})$ based on the assumption.
3) Then calculate Δm.
4) Based on Δm to get the second guess for all the parameters.
5) Repeat the above steps again and again.
The first assumption I made for the three sections is listed in Table. 3.3.

Sections(depth)	P_0	$\sigma(m)$	noise part
1(0-2.79m)	0.1	0.05	0.001
2(2.79m-8.28m)	0.9	0.1	0.0004
3(8.28m-11.76m)	0.9	0.14	0.0001

Table 3.3: The first assumption for three sections

After 100 loops, the ended parameters for the three sections are listed in Tab. 3.4.

Sections	P_0	$\sigma(m)$	noise part
1(0-2.79m)	0.3157	0.0531	0.0013
2(2.79m-8.28m)	0.0825	0.0609	0.00031
3(8.28m-11.76m)	0.1073	0.0833	0.00011

Table 3.4: The final parameters for three sections.

The resulted regression to the power spectrum are shown in Fig. 3.9, 3.10, 3.11. From the three figures, we can see that the regression results for the first three sections are with high quality, and are convincing, and the 90% confidence interval for the three sections are listed in Tab. 3.5, and the regions for 90% are shown in Fig. 3.9, 3.10, 3.11.

Sections		1	2	3
P_0	Upper boundary	0.6407	0.1298	0.0020
	Lower boundary	-0.0187	0.0338	-0.0007
$\sigma(m)$	Upper boundary	0.0657	0.0689	0.0982
	Lower boundary	0.0403	0.0539	0.0685
n	Upper boundary	0.0020	0.0004	0.0002
	Lower boundary	0.0006	0.0002	0.0001

Table 3.5: The 90% confidence interval for three parameters.

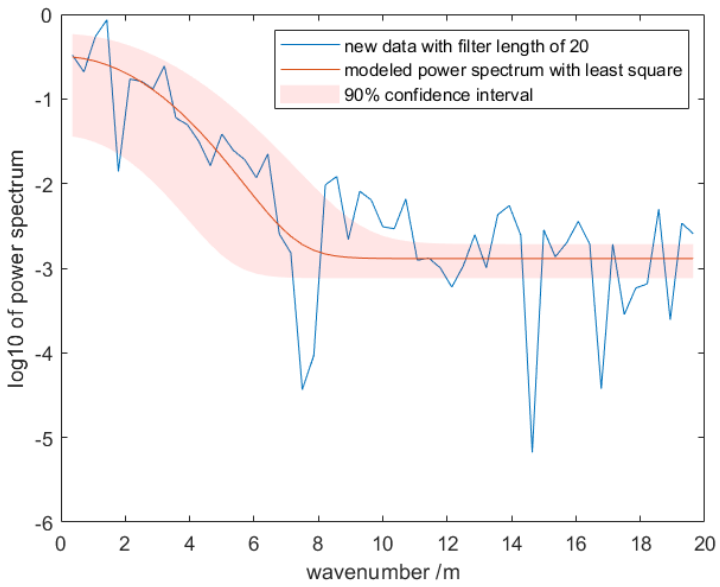

Figure 3.9: The regression for the first section and the region for 90% confidence interval.

From section 3.2, we get the theoretical continuous diffusion length for the ice core, and in this section we get the averaged diffusion length in reality, so we can combine the two results together to have the reasonable diffusion length for the upper 11.76m ice core. And the combined result is shown in Fig. 3.12.

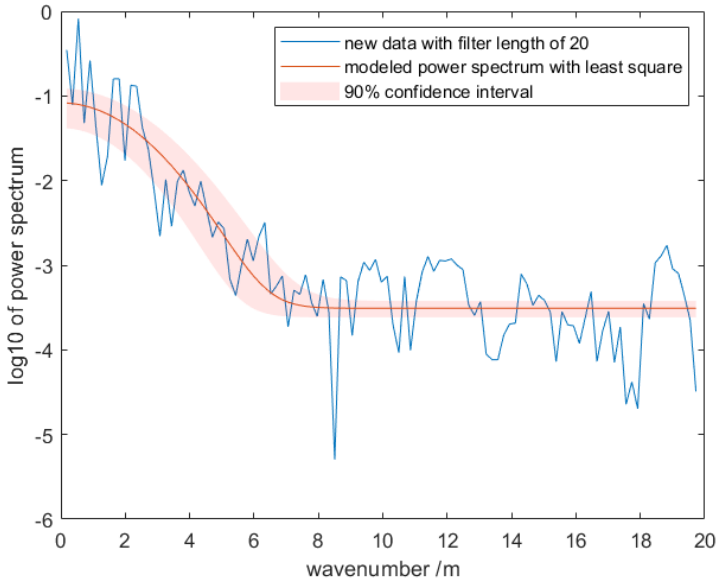

Figure 3.10: The regression for the second section and the region for 90% confidence interval.

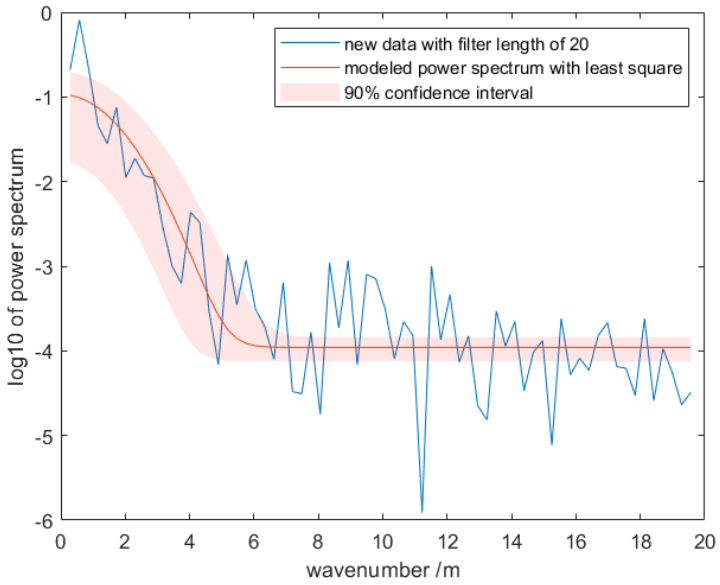

Figure 3.11: The regression for the third section and the region for 90% confidence interval.

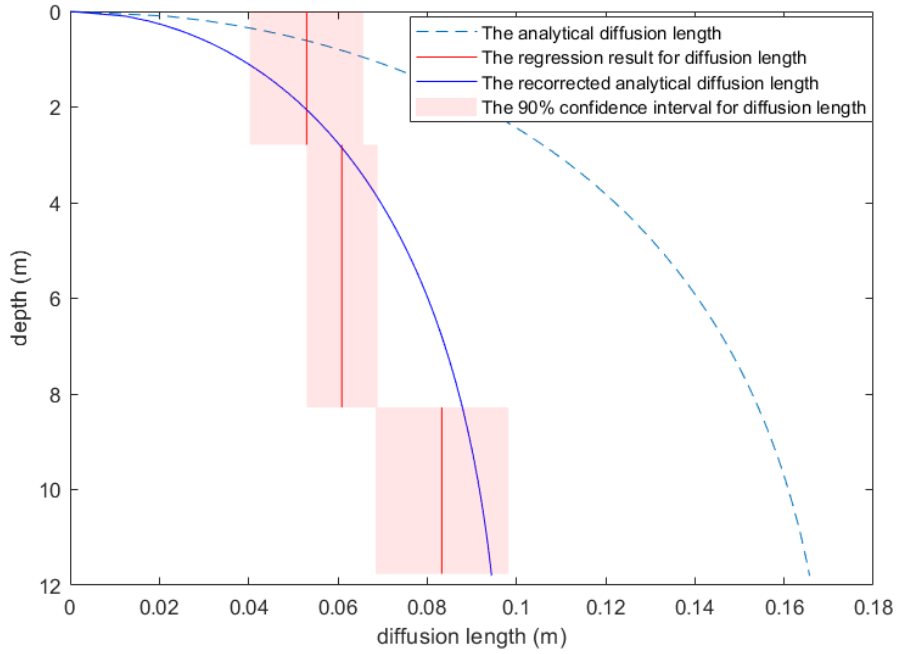

Figure 3.12: The re-corrected analytical diffusion length for the upper 11.76m ice core.

According to the re-corrected analytical diffusion length shown in Fig. 3.12, the final deconvolution result is shown in Fig. 3.13.

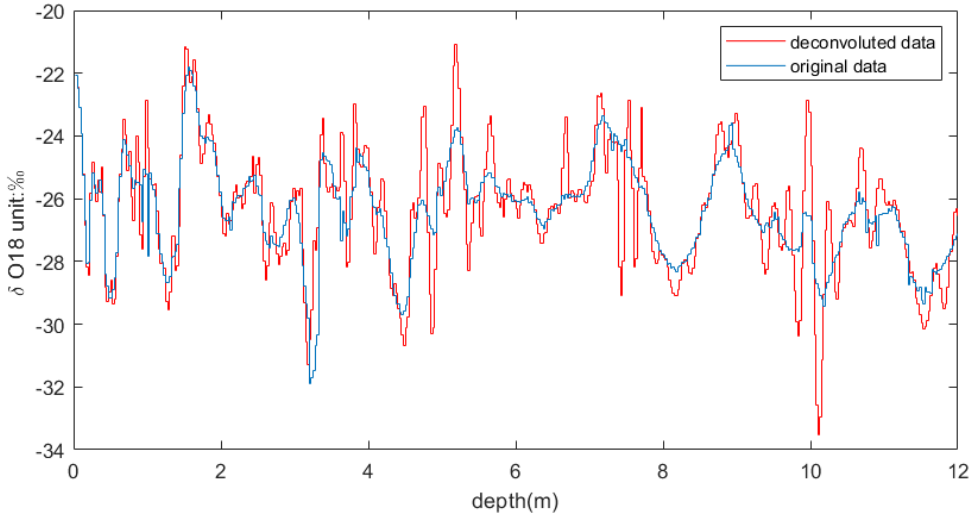

Figure 3.13: The final deconvolution result for isotope data for top 11.76m ice core

4. The Relationship between Isotope Data, Temperature and Accumulation Rate

Now that we have the deconvolution result for the isotope data, we can determine the annual layers based on the cycles in the deconvoluted data. Furthermore we have three reference horizons to decide how many annual layers should be in the interval from 0-11.76m. The depth and its corresponding age year is shown in Tab. 3.1.

As the reference horizons at 11.76m is of higher confidence, we also try to determine the annual layers only based on the 1947 time point, and compare it to the temperature records. Results from the various dating attempts are compared with temperature data from station 4301 and station 4310, including accumulation rate estimates.

4.1 Using the deconvoluted data to calculated annual average $\delta^{18}O$ values

If the year 1947 is at depth of 11.76m, then there should be 49 troughs in this section (Trough in isotope data are interpreted as winters, and as the ice core was drilled in summer 1995, then the winter of 1995 should also be included). The result is shown in Fig. 4.1.

After deciding the annual layers, then we can calculated the yearly averaged isotope data in the deconvoluted version and compare it to the yearly averaged temperature records and seasonal mean temperature records. The correlation coefficients are shown in Tab. 4.1.

From Tab. 4.1

1)The temperature in winter are with the highest correlation coefficients both at station 4301 and 4310, but negatively. And the temperature in spring are with the highest positive correlation coefficients.

2)But for all four seasons and annual averaged temperatures, we can

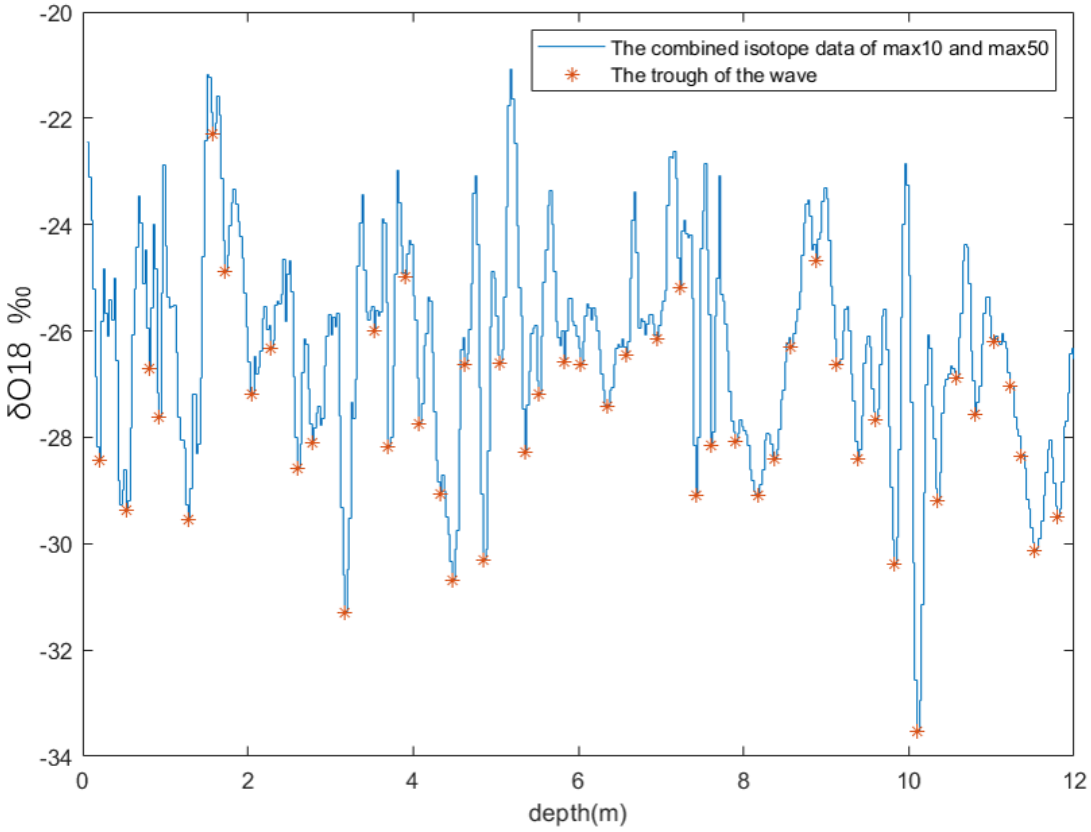

Figure 4.1: The annual layers based on the deconvolution and 1947 time point.

	Spring	Summer	Autumn	Winter	Annual
Dec. $\delta^{18}O$ and 4301	0.1503	0.0603	0.0877	-0.1642	0.0429
Dec. $\delta^{18}O$ and 4310	0.1877	0.0478	0.0773	-0.2023	0.0250

Table 4.1: The correlation coefficients between deconvoluted $\delta^{18}O$ and temperature record at station 4301 and 4310, based on a time scale only taking into account the 1947 reference horizon.

not say that the isotope data is significantly correlated to the temperature records.

4.2 Using the original data to calculate annual average $\delta^{18}O$ values

We can also get the annual averaged isotope data in original isotope data based on the annual layers and compare it to the temperature records. The annual layers in original data is shown in Fig. 4.2.

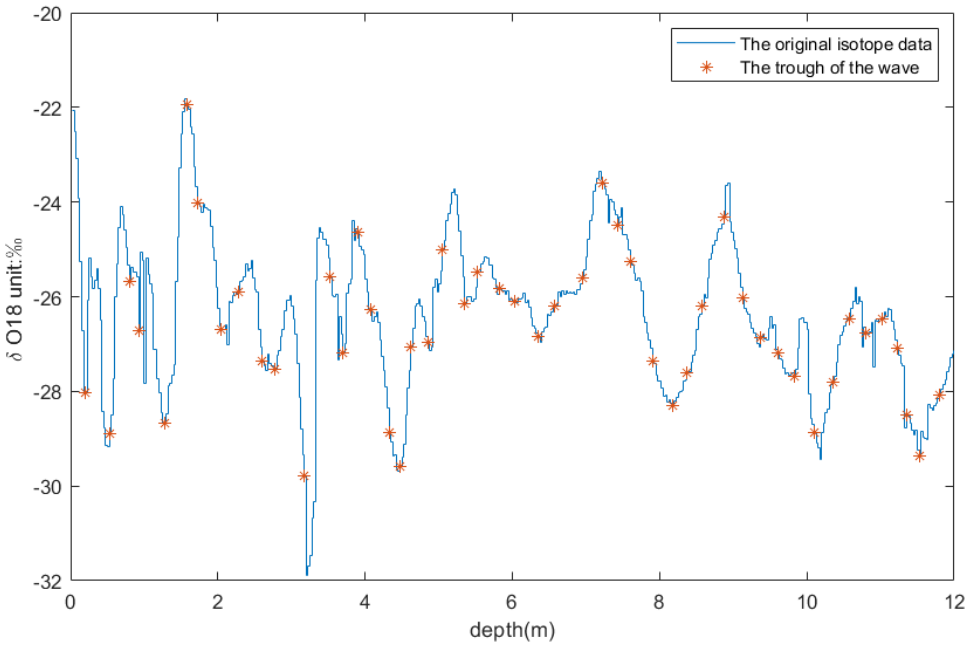

Figure 4.2: The annual layers in original data only based on 1947 time point.

And the correlation coefficients are shown in Tab. 4.2.

	Spring	Summer	Autumn	Winter	Annual
Orig. $\delta^{18}O$ and 4301	0.1363	0.2090	0.0916	-0.1065	0.095
Orig. $\delta^{18}O$ and 4310	0.1494	0.1469	0.0572	-0.1898	0.0343

Table 4.2: The correlation coefficients between original $\delta^{18}O$ and temperature record at station 4301 and 4310.

From Tab. 4.2, we can see that

1) For station 4301, temperature in summer is with the highest correlation coefficients to isotope data, and the correlation coefficients with winter temperature is still negative.

2)But the correlation coefficients are still too low to say that the temperature and isotope data are significantly correlated.

4.3 Including the 1983 and 1963 reference horizons in the dating

Only depending on the 1947 time point can't help us to find the relationship between isotope data and temperature, so we need to try new reference to get new annual layers, and then compare isotope data to temperature record again.

By introducing the 1983 age year, at depth 2.79m, and 1963 age year, at depth 8.28m, I get the new version for annual layer determination, which is shown in Fig.4.3 and Fig. 4.4.

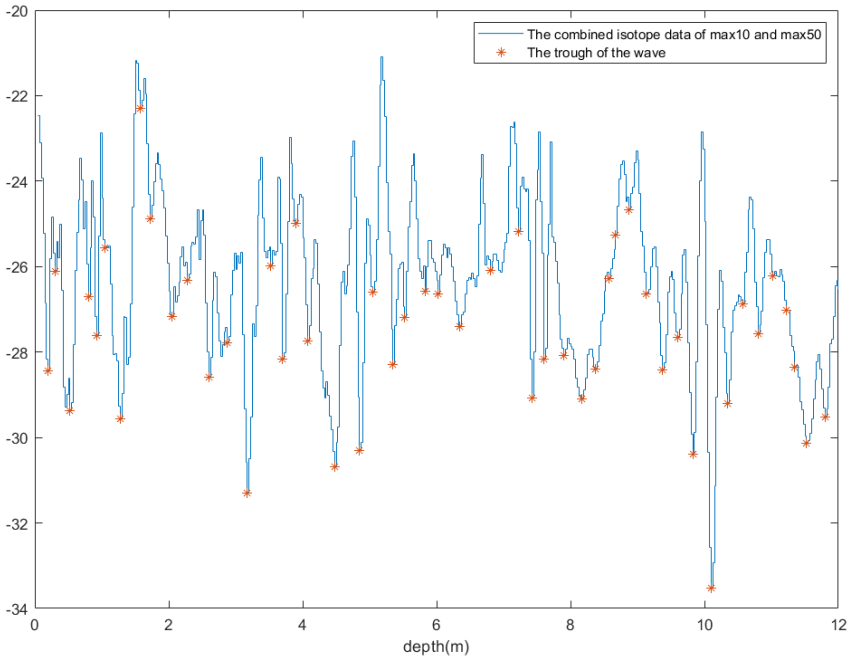

Figure 4.3: The annual layers in the deconvoluted data based on 1983, 1963 and 1947 reference horizons.

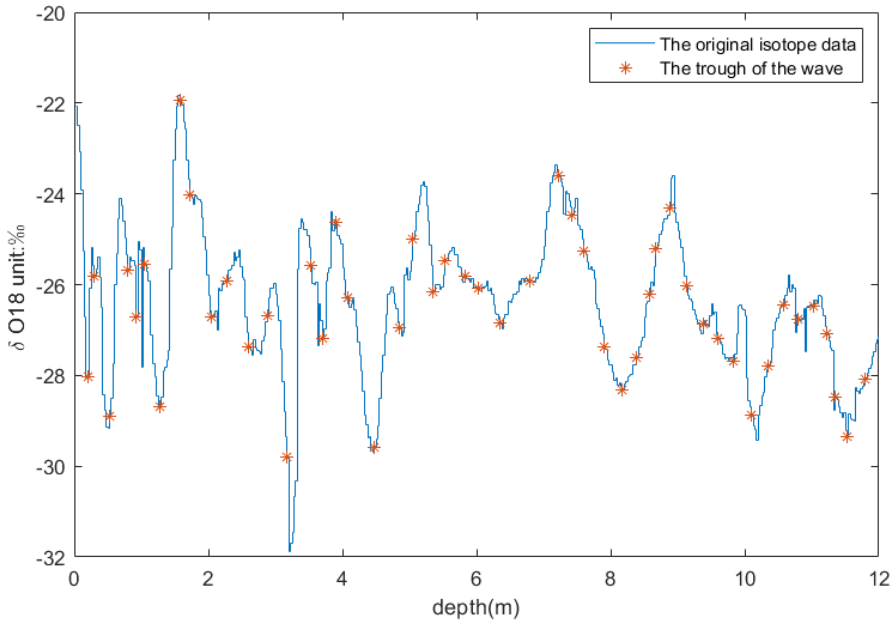

Figure 4.4: The annual layers in original data based on 1983, 1963 and 1947 reference horizons.

And the corresponding correlation coefficients are shown in Tab. 4.3.

	Spring	Summer	Autumn	Winter	Annual
Dec. $\delta^{18}O$ and 4301	0.1495	0.0059	-0.0909	-0.0719	-0.0092
Dec. $\delta^{18}O$ and 4310	0.2326	0.1316	-0.0214	-0.0181	0.1241
Orig. $\delta^{18}O$ and 4301	0.1190	0.0726	-0.1351	-0.1628	-0.0800
Orig. $\delta^{18}O$ and 4310	0.1855	0.0980	-0.1092	-0.1384	-0.0080

Table 4.3: The correlation coefficients between deconvoluted $\delta^{18}O$, original $\delta^{18}O$ and temperature record at station 4301 and 4310.

From Tab. 4.3, we can see:

The correlation coefficients among all the comparison are still so low that we can't say that there is a significant relationship between temperature and isotope data.

So this method can not help us to find the relationship between temperature and isotope data.

4.4 Isotope data , temperature, and accumulation rate

In this section, we are trying to find the relationship between isotope data and accumulation rate. So firstly, we need to determine the accumulation rate from 1947 to 1995.

We can calculate the accumulation rate according to the firn density[9] in the ice core. By transferring the density in ice core to ice density ($920kg/m^3$), and calculating the new volume(length) in ice, we can plot the isotope data in ice depth reference system. And use the annual layer to determine how much ice was stored in one year, which is the accumulation rate. And the isotope data. So the deconvoluted isotope data in ice depth reference system is shown in Fig. 4.5 and Fig. 4.6.

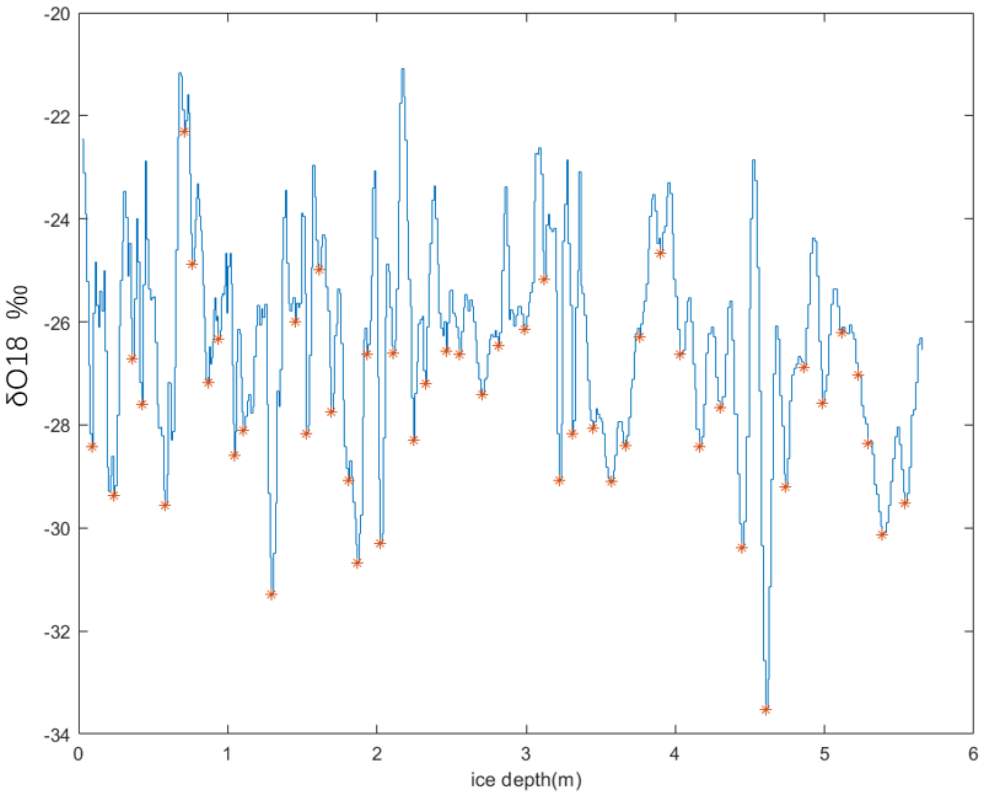

Figure 4.5: The annual layers in deconvoluted data only based on 1947 time point in ice depth under the ice depth reference system.

The calculated accumulation rates in ice are shown in Fig. 4.7.

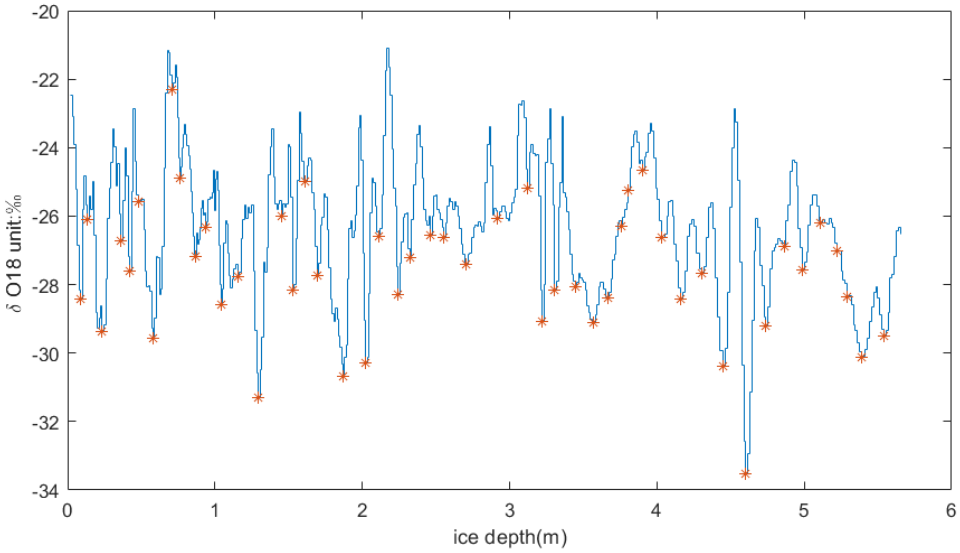

Figure 4.6: The annual layers in deconvoluted data based on 1983, 1963 and 1947 time points under the ice depth reference system.

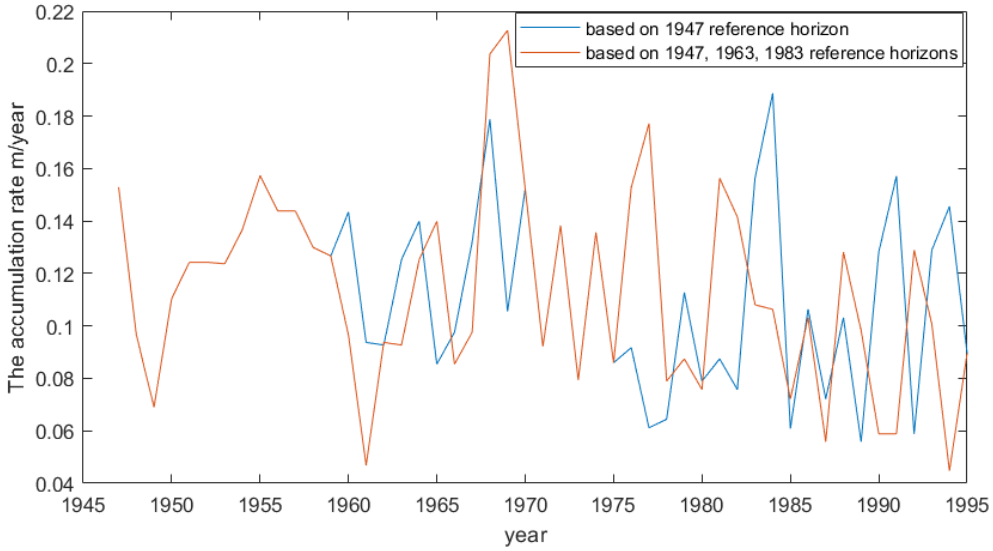

Figure 4.7: The determined accumulation rate.

And the corresponding correlation coefficients between accumulation rate, temperature, and isotope data are shown in Tab. 4.4 and Tab. 4.5.

	Based on 1947	Based on 1983, 1963, 1947
Dec. $\delta^{18}O$ and acc. rate	-0.0454	-0.2706
Orig. $\delta^{18}O$ and acc. rate	-0.0978	**−0.3147**

Table 4.4: The correlation coefficients between deconvoluted $\delta^{18}O$, original $\delta^{18}O$ and accumulation rate. The coefficient with underline means 10% significant level, and coefficient in blackbody means 5% significant level.

		Spring	Summer	Autumn	Winter	Annual
Accu. based on 1947	4301	0.0214	0.0409	0.2255	-0.1277	0.0647
	4310	-0.1564	-0.088	0.1134	0.0724	-0.0090
Accu. based on 1947,1963,1983	4301	-0.1248	-0.2074	0.0302	0.0504	-0.0573
	4310	-0.1740	**−0.3365**	0.1413	0.0256	-0.1014

Table 4.5: The correlation coefficients between accumulation rate and temperature record at station 4301 and 4310. The coefficient in blackbody means 5% significant level.

From Tab. 4.4, we can see that:

Based on 1983, 1963 and 1947 age years to determine the accumulation rate, the isotope data and accumulation rate are significantly negative correlated. If we use deconvoluted isotope data to analyze, then this negative correlation is with 10% significant level. If we use original isotope data to analyze, then this negative correlation is with 5% significant level.

Considering the accumulation rate based on three time points, Tab. 4.5 shows a negative correlated relationship between spring, summer temperature and accumulation rate. Especially at station 4310, the summer temperature and accumulation rate are significantly negative correlated with 5% significant level. But for the accumulation rate only based on the 1947, there is no apparent relationship is shown between temperature and accumulation rate.

So in this section, we get a significant negative correlation between isotope data and accumulation rate, if we retain all three horizons from the original dating and only use the restored data for annual layer counting in between these reference horizons.

5. Discussion

5.1 Temperature

In chapter 2, we developed the continuous temperature records for stations 4301 and 4310, and in this section, we will discuss how our results compare to other Greenland temperature data to have a better understanding of the temperature change in the past tens of years in Greenland.

From Fig. 1.1, we can see that, the temperature rise around the Hans Tausen Ice Cap is between 0.25°C and 0.5°C per decade over 1979-2018 in the ERA-Interim reanalysis. And from data developed in this thesis (Tab. 5.1), at station 4301, from 1979 to 2018, the temperature rise is 1.12°C per decade. Hence the station data suggest a larger rise near Hans Tausen than shown in Fig. 1.1. Therefore the reanalysis does not fully resolve the temperature rise observed near the Hans Tausen Ice Cap. This finding highlights the importance of actual observations. The underestimate of the temperature increase in the reanalysis may be because of 1) A lack of observations used for the reanalysis near Hans Tausen. 2) Local conditions not resolved by the reanalysis.

Station 4310 is in the area with rise 0.5°C-0.75°C per decade, and in our developed data, the rise was 0.71°C per decade, which is in the corresponding reanalysis interval.

Tab. 5.1 shows the decadal annual temperature rise at DMI climate stations 4202, 4211, 4221, 4250, 4272, 4320, 4339, and 4360, as well as the data from stations 4301 and 4310. All stations' positions are labelled in Fig. 5.1. Tab. 5.1 shows that from 1979 to 2018, (except for station 4301), the decadal temperature rise is similar and does not change a lot with latitude. Fig. 5.2 and Fig. 5.3 show the temperature change for these stations, and the extremely high speed rise at station 4301 is clearly seen.

All the stations are along the coast in Greenland. Comparing the observed temperature rise to the result shown in Fig. 1.1, we can see that

1) The observed rise at station 4272 is lower than the reanalysis, which is between 0.75°C and 1°C per decade.

2) The observed rise at station 4339 is also lower than the reanalysis,

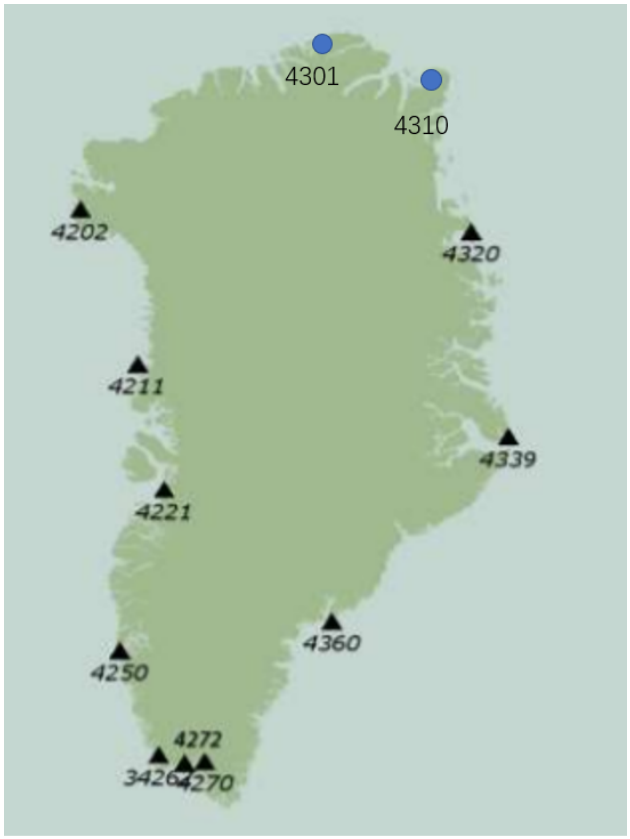

Figure 5.1: The locations for meteorological stations in south and north Greenland. Data from stations indicated with blue circles have been complied in this study.

(Figure adapted from [7])

	4202	4211	4221	4250	4272
Decadal temperature rise °C	0.54	0.79	0.58	0.50	0.47
	4301	4310	4320	4339	4360
Decadal temperature rise °C	1.12	0.71	0.64	0.78	0.72

Table 5.1: The decadal temperature rise from 1979 to 2018 for stations from Greenland.

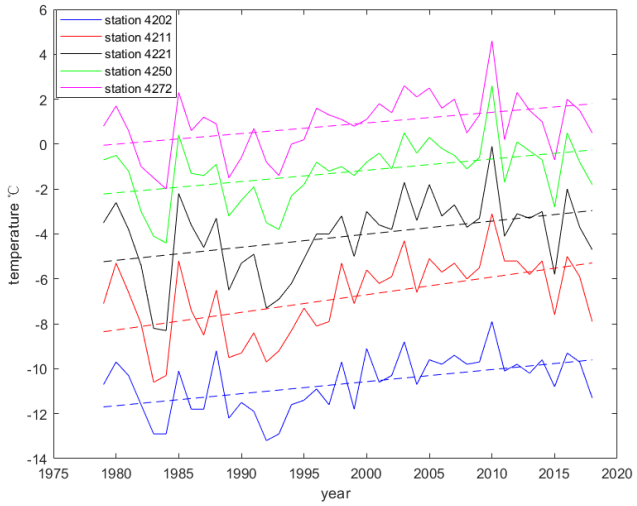

Figure 5.2: The annual temperature averages at stations 4202, 4211, 4221, 4250, 4272 (mainly west coast), and the dashed lines are the corresponding linear regressions used to calculate the rate of temperature change in Tab. 5.1.

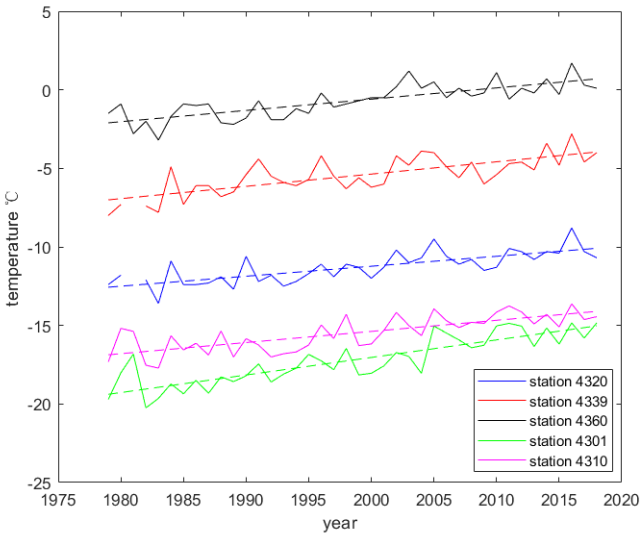

Figure 5.3: The annual temperature averages change at station 4320, 4339, 4360, 4301, 4310(mainly east coast), and the dashed lines are the corresponding linear regression used to calculate the rate of temperature change in Tab. 5.1.

which is over 1°C per decade.

3) Other stations' observed results are in the analysis interval, which are between 0.5°C and 0.75°C per decade.

Fig. 5.4 shows the annual and seasonal surface air temperature trends. From a collection of Arctic stations[5] When we focus on the column covering the period 1979-2008, we can find that the warming speed in winter is faster than the annual speed, and the warming speed in summer is slower than the annual speed in Greenland, which is in agreement with our results in Tab. 2.10 and Tab. 2.11.

The slower warming speed in summer may come from the melting of Arctic sea ice. From Fig. 5.5 and Fig. 5.6, we can see that the anomalies in August changed more than in December, which means that the sea ice decreased more in summer than in winter. So when the sea ice melts in summer, it will absorb much latent heat. And in winter, when new sea ice is formed, then latent heat is released.

5.2 Isotope data

After trying all the methods mentioned in Chapter 4, to restore the water isotope signal in the Hans Tausen Ice Core, we still can not see a clear relationship between isotope data and temperature. We think this result may come from the following reason.

From Tab. 4.5 and Tab. 4.4, we can see a significant negative relationship between accumulation rate and summer temperature, as well as for accumulation rate and isotope data, which means a high summer temperature likely results in a low accumulation for this year, and a high isotope data value is also accompanied with a low accumulation rate.

So a probable reason for the low correlation coefficients between temperature and isotope data is inferred: For a warm year, the precipitation in summer is reduced, but the precipitation in winter is not influenced so much, as a result, the accumulation rate for the whole year becomes low, and the isotope data stored in the ice core is influenced more by the winter precipitation. For a cold year, the precipitation in summer is increased, and the precipitation in winter does not change so much, which result in a high accumulation rate for this year, and the isotope data in the ice core is influenced more by the summer precipitation. So, for some years, the isotope data is influenced more by the winter temperature, for other years, the isotope data is influenced more by the summer temperature. Then the correlation coefficients between isotope data and all the seasonal temperature will be low.

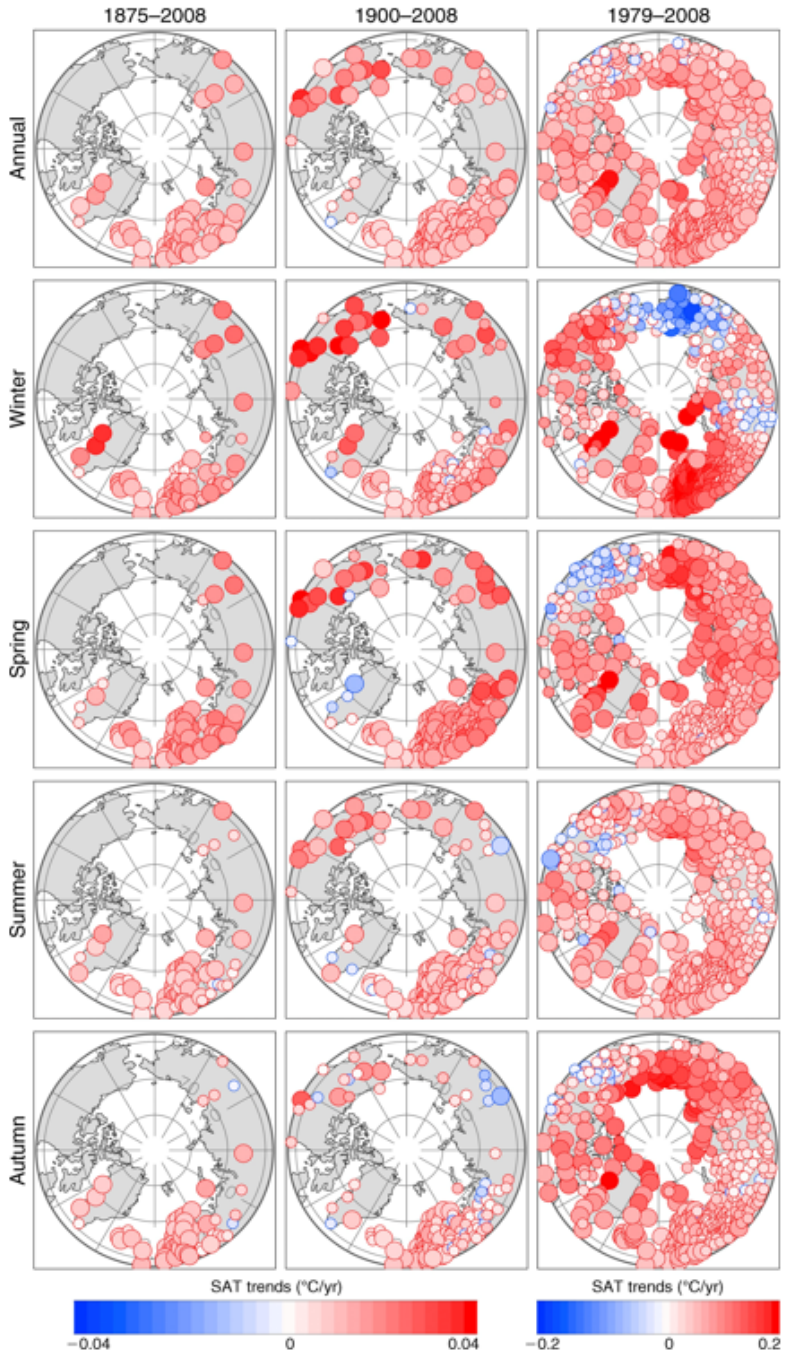

Figure 5.4: Maps of annual and seasonal surface air temperature trends based on meteorological station data. Statistically significant (95% confidence level) trends are marked by larger circles.

(Figure from [5])

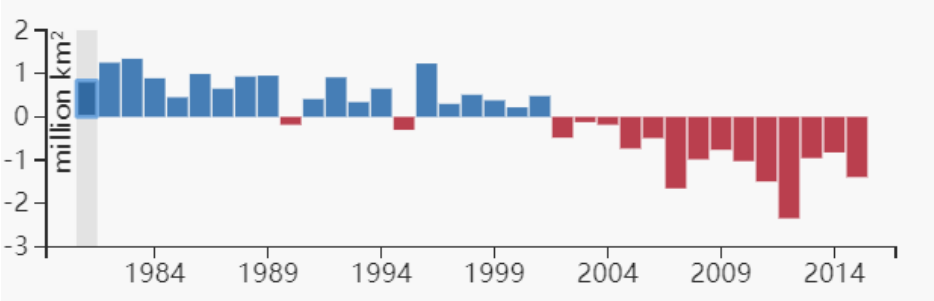

Figure 5.5: Arctic sea ice extent anomalies compared to the average from 1979 to 2015 in August.

(Figure from [3])

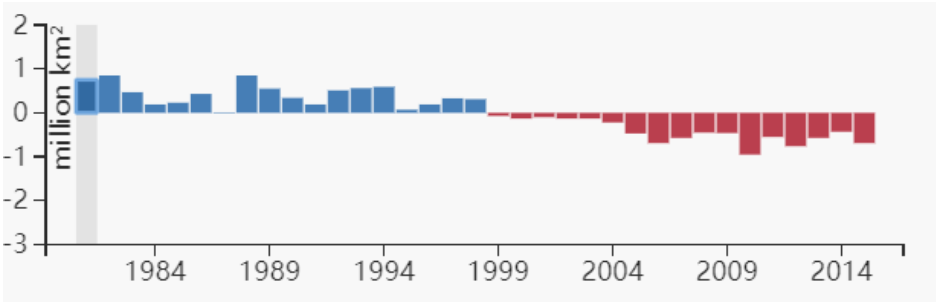

Figure 5.6: Arctic sea ice extent anomalies compared to the average from 1979 to 2015 in December.

(Figure from [3])

The calculated low precipitation associated with high temperature near the Hans Tausen Ice Cap may come from several reasons: 1) Ice melt more induced run off in warm summer. 2) The atmosphere above the Hans Tausen gets dry when temperature is high, maybe due to a Föhn effect caused by the main Greenland Ice Sheet.

The negative correlation between precipitation and temperature shows a dangerous signal for the Hans Tausen Ice Cap, as it means that the ice cap mass balance could be extremely sensitive to the temperature change, meaning the ice will disappear faster as the temperature rises.

Drilling a new shallow core on the Hans Tausen Ice Cap to investigate if this negative relationship between temperature and accumulation persisted in recent decades would be both interesting and valuable.

6. Conclusion

In our study, we mainly developed continuous temperature records at stations 4301 and 4310 from 1951 to 2019, deconvoluted the isotope data to facilitate annual layer counting, and compared the temperature records to the isotope as well as accumulation data to find a relationship between them.

The resulting temperature records at station 4301 and 4310 show a warming trend in northern Greenland, especially after 2000. The warming speed in summer is slower than the annual averaged warming, while the speed in winter is faster than the annual averaged warming. Temperature in the northernmost part of Greenland appear to have increased by more than 1°C per decade since 1979. While most other coastal Greenlandic station show decadal increases in the range 0.5°C-0.85°C.

Under the influence of diffusion and melting, the isotope data stored in the Hans Tausen ice core were degraded. Hence, we firstly removed the melting noise, then did deconvolution to the data to restore the data sufficiently for annual layer counting. The correlation coefficients between Hans Tausen isotope data and temperature observations are low for all seasons as well as for annual averaged temperature. When we compared the isotope data to the accumulation rate estimates, it shows a negative correlation, which means a lower accumulation rate when temperatures are high. This negative relationship explains the low correlation coefficients between isotope data and local temperature record.

Both the temperature record, and the negative correlation between isotope data and accumulation rate show that the Hans Tausen Ice Cap is sensitive to warming. If the temperature keeps rising in the Arctic, the Hans Tausen Ice Cap will likely melt very fast if this effect persists.

Bibliography

[1] Era-interim (european centre for medium-range weather forecast, accessed 9 february 2020). *https://www.ecmwf.int/en/forecasts/datasets/archive-datasets/reanalysis-datasets/era-interim*.

[2] Google map. *https://www.google.com/maps*.

[3] Satellite observations of arctic change. *http://nsidc.org/soac/sea-ice.htmlseaice*.

[4] N. Andersen. On the calculation of filter coefficients for maximum entropy spectral analysis. *Geophysics*, pages 69–72, 1974.

[5] Igor V. Polyakov Bekryaev, Roman V. and Vladimir A. Alexeev. Role of polar amplification in long-term surface air temperature variations and modern arctic warming. *Journal of Climate*, pages 3888–3906, 2010.

[6] Herron M. M.; Langway C. C. Firn densification: an empirical model. *Journal of Glaciology*, pages 373–385, 1980.

[7] John Cappelen. Greenland - dmi historical climate data collection 1784-2019. *DMI Report 20-04*, pages 1–119, 2020.

[8] John Cappelen. Weather observations from greenland 1958-2019 - observation data with description. *DMI Report 20-08*, pages 1–33, 2020.

[9] Henrik B. Clausen; et. al. Glaciological and chemical studies on ice cores from hans tausen iskappe, greenland. *The Hans Tausen Ice Cap. Glacialogy and glacial geology*, pages 123–149, 2000.

[10] S. J. Johnsen; et. al. Diffusion of stable isotopes in polar firn and ice: the isotope effect in firn diffusion. *Physics of Ice Core Records*, pages 121–140, 2000.

[11] Dee D. P.; et.al. The era-interim reanalysis: configuration and performance of the data assimilation system. *Q. J. Roy. Meteor. Soc. 137*, page 553–97., 2011.

[12] Eystein Jansen; et.al. Past perspectives on the present era of abrupt arctic climate change. *NATURE CLIMATE CHANGE*, 2020.

[13] Peter U. Clark; et.al. Consequences of twenty-first-century policy for multi-millennial climate and sea-level change. *NATURE CLIMATE CHANGE*, 2016.

[14] S. J. Johnsen. Stable isotope homogenization of polar firn and ice. *Isotopes and impurities in snow and ice*, pages 210–219, 1977.

[15] Dansgaard W et al. Johnsen S J, Clausen H B. Irregular glacial interstadials recorded in a new greenland ice core. *Nature*, pages 311–313, 1992.

[16] Anker Weidick Jon Y. Landvik and Anette Hansen. The glacial history of the hans tausen iskappe and the last glaciation of peary land, north greenland. *The Hans Tausen Ice Cap. Glacialogy and glacial geology*, pages 27–44, 2000.

[17] C.C Langway. Accumulation and temperature on the inland ice of north greenland. *Journal of Glaciology 3 (30)*, pages 1017–1044., 1959.

[18] Matthew J. Menne; Claude N. Williams; Byron E. Gleason; J. Jared Rennie; Jay H. Lawrimore. The global historical climatology network monthly temperature dataset, version 4. *Journal of Climate*, pages 9835–9854, 2018.

[19] Vinther B M. Seasonal 18o signals in greenland ice cores[j]. *Master's thesis, University of Copenhagen, Denmark*, 2003.

[20] Jouzel J Merlivat L. Global climatic interpretation of the deuterium-oxygen 18 relationship for precipitation. *Journal of Geophysical Research: Oceans*, pages 5029–5033, 1979.

[21] Reeh N. Report on activities and results 1993-1995 for hans tausen ice cap project – glacier and climate change research. *Report to the Nordic Minister Council*, page 52pp, 1995.

[22] Reeh N.; O. Olesen; H. H. Thomsen; W. Starzer and C. E. Bøggild. Mass balance paramerization for hans tausen iskappe, peary land, eastern

north greenland. *Meddelelser om Grønland, Geoscience 39*, pages 57–69, 2001.

[23] Bo M. Vinther. A matlab routine for spectrally consistent gap-filling in data series. 2019.

[24] Anker Weidick. Neoglacial glaciations around hans tausen iskappe, peary land, north greenland. *The Hans Tausen Ice Cap. Glacialogy and glacial geology*, pages 5–26, 2000.